

ALMA MATER STUDIORUM · UNIVERSITÀ DI BOLOGNA

---

**SCUOLA DI INGEGNERIA E ARCHITETTURA**

*DIPARTIMENTO DI INGEGNERIA CIVILE, CHIMICA, AMBIENTALE E DEI MATERIALI -  
DICAM*

*MATERIALS AND SENSOR ENGINEERING FOR ENVIROMENTAL SUSTAINABILITY*

**TESI DI LAUREA**

in  
Nanotechnology

**DIELECTROPHORESIS (DEP) AND ELECTROWETTING (EWOD)  
AS AN ANTI-FOULING PROCESS  
FOR ANTIBACTERIAL SURFACES**

**CANDIDATO:            RELATORE:**

Alberto Stavros  
Yika Tuesta

Chiar.mo Prof. Ferruccio Doghieri

**CORRELATORI:**

Prof. Wouter van der Wijngaart

Dott. Fredrik Carlborg

**2012/13  
III Sessione**



## Abstract

La ricerca odierna in campo medico si focalizza sulla diminuzione della formazione di biofilm batterici in grado di portare l'insorgere di infezioni. La sterilizzazione di dispositivi biomedicali non cambia per un lungo periodo di tempo. Questo si traduce in costi elevati per le gestioni sanitarie dell'ospedale. L'obiettivo di questo progetto è quello di studiare gli effetti dei campi elettrici e la manipolazione dell'energia superficiale come soluzioni per prevenire la formazione di batteri sui biofilm presenti nei dispositivi futuri.

Partendo da un ambiente elettrocinetico sono stati testati due diversi metodi: fattibilità di gradiente elettrico attraverso i medium (DEP) rinforzata da simulazioni numeriche; e EWOD dalla fabbricazione di elettrodi interdigitati d'oro su substrati di vetro siliceo, strato standard di  $\sim 480$  nm di Teflon (PTFE) e guarnizione polimerica per contenere il mezzo di batteri.

Il primo esperimento riguarda l'analisi quantitativa ed è stato realizzato per ottenere l'azione necessaria per allontanare i batteri, senza considerare limitazioni dell'ambiente dielettrico come dipendenza di batteri e mezzo dalla frequenza elettrica. Nel secondo esperimento di tensioni applicate, è stato caratterizzato dalle misure di angolo di contatto delle goccioline per mettere alla prova batteri vivi.

Il progetto ha portato a risultati promettenti per l'applicazione DEP grazie alla sua ampia gamma di frequenze che possono essere utilizzate per avere un rigetto "generale" dei batteri, ma in termini di praticità, EWOD probabilmente ha una maggiore possibilità di successo. Saranno comunque necessari più esperimenti per verificare se si potrà impedire l'adesione dei biofilms, senza considerare le proprietà non-adesive del Teflon (comprese le limitazioni: come Teflon sfondamento, sensibilità di strato) per tempi di incubazione più elevate di 24 ore.

## Abstract

Nowadays the medical field is struggling to decrease bacteria biofilm formation which leads to infection. Biomedical devices sterilization has not changed over a long period of time. This results in high costs for hospitals healthcare managements. The objective of this project is to investigate electric field effects and surface energy manipulation as solutions for preventing bacteria biofilm for future devices.

Based on electrokinetic environments 2 different methods were tested: feasibility of electric gradient through mediums (DEP) reinforced by numerical simulations; and EWOD by the fabrication of golden interdigitated electrodes on silicon glass substrates, standard  $\sim 480$  nm Teflon (PTFE) layer and polymeric gasket to contain the bacteria medium.

In the first experiment quantitative analysis was carried out to achieve forces required to reject bacteria without considering dielectric environment limitations as bacteria and medium electric frequency dependence. In the second experiment applied voltages was characterized by droplets contact angle measurements and put to the live bacteria tests.

The project resulted on promising results for DEP application due to its wide range of frequency that can be used to make a “general” bacteria rejecting; but in terms of practicality, EWOD probably have higher potential for success but more experiments are needed to verify if can prevent biofilm adhesion besides the Teflon non-adhesive properties (including limitations as Teflon breakthrough, layer sensitivity) at incubation times larger than 24 hours.

## **Abbreviations**

**AC** Alternate current

**CA** Contact angle

**CM** Clausius-Mossotti

**DC** Direct current

**DEP** Dielectrophoresis

**EDL** Electrical Double-Layer

**EP** ElectroPhoresis

**EW** ElectroWetting

**EWOD** ElectroWetting-on-Dielectric

**HCAI** Healthcare Associated Infections

**M9** M9 minimal medium - minimal microbial growth medium

**nDEP** negative DEP

**OSTE** off-stoichiometry thiolene

**PDMS** PolyDimethylSiloxane

**PBS** Phosphate buffered saline

**pDEP** positive DEP

**PR** PhotoResist

**UV** Ultraviolet(UV) light

**VRI** Viral respiratory infections

**WHO** World Health Organization

# Contents

|          |   |           |
|----------|---|-----------|
| <b>1</b> | <b>Introduction</b>   | <b>8</b>  |
| 1.1      | Project Definition & Goals - Motivation . . . . .                       | 8         |
| 1.2      | Hypothesis Theory . . . . .   | 10        |
| <b>2</b> | <b>Background and State of Art</b>                                      | <b>11</b> |
| 2.1      | Biofilm formation and prevention . . . . .                              | 11        |
| 2.2      | Theory themes (DEP-EWOD) . . . . .                                      | 13        |
| 2.2.1    | Dielectrophoresis Force . . . . .                                       | 14        |
| 2.2.2    | Dielectrophoresis in DC and AC Fields . . . . .                         | 15        |
| 2.2.3    | EWOD in Direct current (DC) and Alternate current (AC) fields . . . . . | 16        |
| 2.2.4    | Theory limitations . . . . .  | 17        |
| 2.3      | Modelling of biological cells . . . . .                                 | 17        |
| 2.3.1    | Biological cells on DEP . . . . .                                       | 17        |
| 2.3.2    | Hydrophobic effect on bacteria adhesion . . . . .                       | 19        |
| 2.4      | Modelling of electrodes . . . . .                                       | 19        |
| <b>3</b> | <b>Design and assembly of the experimental setup</b>                    | <b>21</b> |
| 3.1      | Chip design and assembly . . . . .                                      | 21        |
| 3.1.1    | Electrode design . . . . .  | 21        |
| 3.1.2    | Chip fabrication . . . . .  | 23        |
| 3.2      | Gasket fabrication . . . . .  | 33        |
| 3.2.1    | Gasket version 1 . . . . .  | 33        |
| 3.2.2    | Gasket version 2 . . . . .  | 38        |
| 3.2.3    | gasket tests . . . . .  | 39        |
| 3.3      | Bacteria to be used . . . . .   | 41        |
| 3.3.1    | Salmonella Typhimurium . . . . .  | 41        |
| <b>4</b> | <b>Measurements and results</b>   | <b>43</b> |
| 4.1      | Numerical simulations of DEP on bacteria model . . . . .                | 43        |
| 4.1.1    | MATLAB calculations . . . . .   | 43        |
| 4.1.2    | COMSOL analysis and results . . . . .                                   | 46        |
| 4.2      | Experiments of EWOD surfaces on live bacteria . . . . .                 | 52        |
| 4.2.1    | Contact angle tests . . . . .   | 52        |
| 4.2.2    | Waveform tests . . . . .  | 55        |
| 4.3      | Bacteria tests . . . . .  | 55        |

## CONTENTS

---

|  |           |
|--|-----------|
| 4.4 Discussion . . . . .                             | 59        |
| <b>5 Conclusion</b>                                  | <b>62</b> |
| 5.1 Project summary . . . . .                        | 63        |
| 5.2 Outlook . . . . .                                | 63        |
| <b>A Biofilm on hospital environments challenges</b> | <b>68</b> |
| <b>B MATLAB Program</b>                              | <b>70</b> |
| B.1 Command set . . . . .                            | 70        |
| <b>C COMSOL simulations</b>                          | <b>73</b> |
| <b>D Bacteria formation</b>                          | <b>74</b> |
| D.1 Bacteria . . . . .                               | 74        |
| D.2 Medium . . . . .                                 | 75        |
| <b>E OSTE tests detailed information</b>             | <b>76</b> |
| E.1 Material specification . . . . .                 | 76        |
| <b>F Chip fabrication detailed information</b>       | <b>77</b> |
| F.1 Design / L-EDIT . . . . .                        | 77        |
| F.2 Procedures . . . . .                             | 78        |
| F.3 Parameters . . . . .                             | 79        |
| <b>G EWOD attempts</b>                               | <b>81</b> |

# List of Figures

|      |   |    |
|------|---|----|
| 2.1  | Commercial Electrode-gasket sample for cells and/or proteins . . . . .        | 11 |
| 2.2  | Attachment of bacteria cells mechanism . . . . .                              | 13 |
| 2.3  | DEP variations by its applications . . . . .                                  | 13 |
| 2.4  | Effect of $\vec{E}$ on particle . . . . .                                     | 15 |
| 2.5  | Interdigitated electrode distance effect on Electric field[1] . . . . .       | 16 |
| 2.6  | DEP cell modelling[2] . . . . .   | 18 |
| 2.7  | Hydrophobicity and attach cell number (RP62A) relationship . . . . .          | 19 |
| 2.8  | Different existing Dielectrophoresis (DEP) devices classification . . . . .   | 20 |
| 2.9  | ElectroWetting (EW) electric fields and equivalent Electric circuit . . . . . | 20 |
| 3.1  | Electrodes configuration . . . . .  | 22 |
| 3.2  | Electrodes in square spaces . . . . .   | 23 |
| 3.3  | Mask and expectable wafer design . . . . .                                    | 24 |
| 3.4  | Wafer structure layers . . . . .  | 25 |
| 3.5  | Process of Photo-lithography . . . . .  | 26 |
| 3.6  | Teflon technique to insulate on only electrodes . . . . .                     | 29 |
| 3.7  | Metal Mask Measurements . . . . .   | 30 |
| 3.8  | Diced finished wafer . . . . .  | 31 |
| 3.9  | Final built test device . . . . .   | 31 |
| 3.10 | Etching time problem . . . . .  | 32 |
| 3.11 | Electrode bad etching finish . . . . .  | 32 |
| 3.12 | Commercial gasket and design . . . . .  | 33 |
| 3.13 | OSTE gasket on aluminium mould . . . . .                                      | 35 |
| 3.14 | One hole gasket designs . . . . .   | 36 |
| 3.15 | One hole gasket procedure . . . . .   | 37 |
| 3.16 | Different made PolyDimethylSiloxane (PDMS) gaskets . . . . .                  | 38 |
| 3.17 | OSTE and PDMS gaskets on sealing tests . . . . .                              | 40 |
| 3.18 | Salmonella typhimurium . . . . .  | 42 |
| 4.1  | Excel & Matlab CM plots . . . . .   | 45 |
| 4.2  | CM on diff. mediums . . . . .   | 46 |
| 4.3  | Electric potential intensity . . . . .  | 47 |
| 4.4  | Electric Field intensity . . . . .  | 47 |
| 4.5  | DEP Force . . . . .   | 48 |
| 4.6  | COMSOL DEP simulation - Electric field analysis . . . . .                     | 50 |



## LIST OF FIGURES

---

|      |  |    |
|------|--|----|
| 4.7  | EWOD setup for Contact angle (CA) measurements . . . . .   | 52 |
| 4.8  | CA by evaporation . . . . .                                | 53 |
| 4.9  | CA within different voltages . . . . .                     | 54 |
| 4.10 | Waveform tests . . . . .                                   | 55 |
| 4.11 | Setup used for bacteria tests . . . . .                    | 56 |
| 4.12 | Electrodes' cells numbered and labelled . . . . .          | 56 |
| 4.13 | Bacteria tests stages . . . . .                            | 57 |
| 4.14 | Droplet CA change & electrolysis . . . . .                 | 60 |
| 4.15 | Bacteria tests on with interdigitated electrodes . . . . . | 61 |
|      |  |    |
| C.1  | DEP forces at different heights . . . . .                  | 73 |
|      |  |    |
| D.1  | Bacteria biofilm matrix forces . . . . .                   | 74 |
|      |  |    |
| F.1  | Different electrodes topology . . . . .                    | 77 |
| F.2  | Electrode design attempt . . . . .                         | 78 |
|      |  |    |
| G.1  | EWOD variety test . . . . .                                | 81 |

# List of Tables

|      |  |    |
|------|--|----|
| 1.1  | Costs of breeding ground for antibiotic resistant bacteria[3]                                | 9  |
| 3.1  | Different width of the electrode depending on the case used                                  | 22 |
| 3.2  | Photoresist curing time parameters   | 25 |
| 3.3  | Different used etching times on lithography  | 27 |
| 3.4  | Spindle and Feed speeds for the different materials  | 27 |
| 3.5  | Glass Blade parameters   | 28 |
| 3.6  | Silicon Oxide Blade parameters   | 28 |
| 3.7  | OSTE Formulation: Stoichiometry, monomers and curing agent                                   | 34 |
| 3.8  | PDMS Formulation: base and curing agent ratio  | 38 |
| 3.9  | Curing time for 2mm OSTE   | 39 |
| 3.10 | Curing time for 1mm OSTE   | 40 |
| 4.1  | Three-layer particle parameters  | 44 |
| 4.2  | DEP force calculated from COMSOL simulations   | 51 |
| 4.3  | Drift velocity for different bacteria  | 51 |
| 4.4  | Diffusion length of bacteria during one second   | 51 |
| 4.5  | Bacteria adhesion tests done in Karolinska laboratories                                      | 58 |
| D.1  | M9 medium parameters   | 75 |
| E.1  | Culture plate parameters   | 76 |
| F.1  | UV exposure and development times - Second lithography attempt with standard softbake(110°C) | 79 |
| F.2  | UV exposure and development times - Second lithography attempt with lower softbake(90°C)     | 79 |
| F.3  | Measurements of the electrodes and gaps in the second attempt from Tab.F.2                   | 79 |
| F.4  | Dicing blade parameters about the used Flange  | 80 |

# Chapter 1

## Introduction

The aim of this part is to introduce the topic and explain in further details the project definition, goals and the motivation behind it.

### 1.1 Project Definition & Goals - Motivation

From ancient times until nowadays the demand of antibacterial surfaces has been present and there is still a latent solution. The main area of need is in hospital environments, where 80% of most common nosocomial infection are associated to urinary catheters[4].

The purpose of this project is to investigate how electrokinetic microenvironments affects bacteria adhesion, specifically with the interaction of electric fields gradient, and surface dielectric capacitance in an array of interdigitated electrodes.

The practical motivation behind the project was to investigate possible solutions for preventing bacteria biofilm formation in healthcare devices, such as on joint prosthesis (orthopaedic), on urinary catheters and on airways intubation tubes, where bacteria become the cause of Healthcare Associated Infections (HCAI) and Viral respiratory infections (VRI).

Previously all approaches to prevent health care related infections have centred around removing or killing the bacteria adhering on the surface of the devices. These have several drawbacks such as eventual build up of a biofilm consisting of dead bacteria and/or long term negative effects such antibiotic resistance caused by catheters coated with antibiotic substances. Instead the electrokinetic approach investigated in this thesis focuses on creating a sufficiently unattractive environment on the surface as to completely prevent bacteria from attaching.

**Hospital environment challenges** From the beginning of the ages, infectious diseases were the major cause of death on mankind until antimicrobials were discovered. Nowadays, places where healthcare is not well supported are still struggling with deaths caused by infections and in more supported healthcare places antimicrobial resistance is the major cause of deaths making antibiotics practically ineffective.

From the public health point of view, this represents high costs and hospital-related infection by highly resistant bacteria, which is not a disease but a misused way of healthcare practices.

The main problem of antimicrobial resistance is the total dependence for treating infections, new methods to avoid microbial cannot avoid the antimicrobial resistance itself but

## 1.1 Project Definition & Goals - Motivation

---

contribute to release it from be the most important public health concern[5].

At the moment one of the major problems can be the time, money and logistic invested in the use of disinfectants in hospital environments as can be seen on Table 1.1.

| Hospital-acquired Infections | Costs (US\$)           |
|------------------------------|------------------------|
| USA                          | \$10 billion per year  |
| Mexico                       | \$450 million per year |
| Thailand                     | \$40 million per year  |

Table 1.1: Costs of breeding ground for antibiotic resistant bacteria[3]

Bacteria can survive several days, and the only way to reduce biofilm formation is cleaning and disinfecting the used surfaces. Time to inactivate virus can go from 5 minute to more than one day depending on the concentration of the inoculation and the disinfectant dilution shown in Table1 and Table2 from severe acute respiratory syndrome (SARS) survival method[6].

Reusable medical devices that are in continuous mucous contact should receive high-level disinfection (explained further in section A) between different patients (including endoscopes, ETT {Endotracheal Tube or Breathing Tube}, anaesthesia circuits, and ventilators). In addition to it, some prosthetics or inner devices needed chemical sterilization instead of high temperature sterilization due to the material degradation; and the antiseptics themselves also are sensitive to store and transportation conditions, which in humans can produce sensitive reactions as well depending in the administrative doses (further chemical agents specifications can be found in section A in the appendix).

In the other hand, what happened if this antibiotic dependence ends? There have been an incredible reduce of use in antibiotics in the EU countries due to a ban on some of the antimicrobial growth promoters (AGP), which reduce antibacterial resistance on food. This ban results in imported generic products to replace the needed antimicrobial to be used in farms. And a more prudent education should have been needed to perform to producers and veterinarians.[7]

In the USA, 5-10% of hospital patients suffers healthcare-associated infections (HAIs), where the most relevant of them are urinary tract infections related to catheter in the 35% of the cases.

In invasive operations (such as Sectio caesarea) antimicrobial prophylaxis is needed to be administrated 60 min prior it, at a right bacterial concentration. This always reduces the incidences of infections. Biofilm, mainly in endotracheal tubes is eliminated mechanically or by silver coating.

**Antimicrobial resistance** From ancient periods of time Microorganisms defence from other microorganisms has been to produce their own chemical substances, this are called nowadays as antibiotics or antimicrobial agents.

Fortunately not all become resistant to other's antibiotics. In our body, this can be forced by the effect of antibiotics in our system that expand our resistant strains making of us more vulnerable, or by transmission of resistance microbes that lives on other's patients systems, like in hospitals environments. Antimicrobial resistance is mainly driven by healthcare practices, where antimicrobial are overdosed in patients who does not need exactly that as refereed in

[8],[4].

A multi-drugresistant organism (MDRO) are very common mainly resistant to fluoroquinolones [9].

## 1.2 Hypothesis Theory

Selective methods to manipulate particles (included bacteria) can be used. In this case, electrical fields can be applied into a medium to move submerged particles in it(just like bacteria biofilm).

These methods are: ElectroPhoresis (EP), DEP and EW. Further details are presented in Section2.2. For instance DEP can exert enough forces into particles depending on the dielectric values and of its medium too. This rely on a very wide range of frequency which defines an attraction force or repulsive from the surface. Hence bacteria biofilm can be keep away from surface, make its adherence unsettled.

In the other hand, ElectroWetting-on-Dielectric (EWOD) can create particle displacement as it can be done with liquid droplets depending on the applied voltage and the thickness of the dielectric layer on top of the surface. Therefore bacteria biofilm can be not only rejected from adhesion but capable of be manipulated and transported along the surface.

## Chapter 2

# Background and State of Art

In this chapter anti-biofouling technologies history is reported. Furthermore, the theory themes behind the experiments are presented. Additionally, this chapter provides a basic theory about EW and DEP.

Also illustrates how physics works on these postulates, making the reader being aware of what this theories implies.

About electrode-gasket methods, there are already some samples of Disposable Electrode Arrays built and commercialized like in Fig2.1, which are able to interact between cell proteins, and make cell proliferation measurements[10].

Moreover, it can be found also in the market antimicrobial-impregnated central venous catheter which use two antiseptics(chlorhexidine and silver sulfadiazine) to avoid bacteria colonization, which has been used in transplants, septic patients (included burned patients)[11].

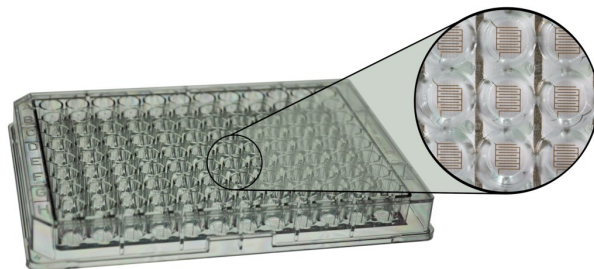


Figure 2.1: Electrode-gasket sample for Cell-extracellular matrix (ECM) protein interactions, signal transduction assays,detection of invasion of endothelial cell layers by metastatic cells, barrier function measurements and cell proliferation applications[10]

### 2.1 Biofilm formation and prevention

Surfaces have an important role in the micro-organism activity; biofilm formation is formed as a defence from adverse conditions (low nutrients, extreme temperatures).

Adherence to the surface happens by the secretion of extracellular polysaccharide substance

from cells (known as slime). All in all, microbial biofilms tends to be a complex heterogeneous microbial ecosystem.

The biofilm formation sequence starts with the conditioning of the surface, followed by the colonisation of the bacteria and finally its multiplications. This microenvironment can be changed to expansion, either by the removal of microcolonies parts and future growth in farther places, or increased by fluids flows that carries nutrients. In both cases the growth aiding is always positive.

Biofilm's structure is very similar to a pile of Lego® pieces where bacteria can overlapped each other in different spots and orientations, making easy to interconnect themselves by its flagella and cellulose (like bricks and cement) in a common secretion medium. By this, bacteria is allowed to breath and be protected from outer biocides. But not all organisms on biofilm have been recognised yet. Factors that increased the formation come from nutrients presence, to warm temperature, and flows stagnation on fluids channel dead-ends[12].

**Microbial adhesion mechanism, DLVO theory** In a dielectric medium, ions are dispersed all over it. But there will be a gradient of ions density where a interface is contained. For example, when a charged particle is introduced in this medium counter ions begin to screen all over its surface by self-organization manner however not in an uniform way. In fact, counter ions structured in layers with different characteristics which behaviour is explained through Debye-Hückel theory, mathematical formula derived from Poisson equation[13].

This is called Debye screening effect[14]. The first layer is always composed of the attached counter ions; this together with the ions behind the interface forms the so called Stern layer[15] which is located in the Inner Helmholtz Plane (IHP). The second layer is composed of a diffuse ion layer, which is attached by Coulomb forces. This two equalled opposite charged layers are defined as an Electrical Double-Layer (EDL). It is important to consider the distance that ions affect beyond the EDL, which is called Debye Length, for phosphate-buffered saline (PBS) is 0.7nm.

The kinetic stability between energy interactions of particles is explained by Derjaguin-Landau-Verwey-Overbeek (DLVO) theory[13]. This theory combined the van der Waals attraction forces and the electrostatic repulsion forces at low surface potentials (potential energy  $\ll$  thermal energy) considering EDL limits[16].

First, bacteria cell is transported to the surface by sedimentation forces and hydrodynamic forces (drag force), until reaching the Diffusive boundary layer illustrated in Fig2.2. At this point the only main force is the diffusion, where its diffusion transportation behaviour is purely by Brownian motion; here DLVO forces are present between surface and the bacteria cell. However, the cell attachment is reversible due to still week surface interaction. This interaction range is relative small ( $< 1\mu\text{m}$ ), where both surfaces present negative charges until EDL is overcome. Finally stronger irreversible forces arrived at attachment where its range begins from 5 to several hundreds of nanometers[17].

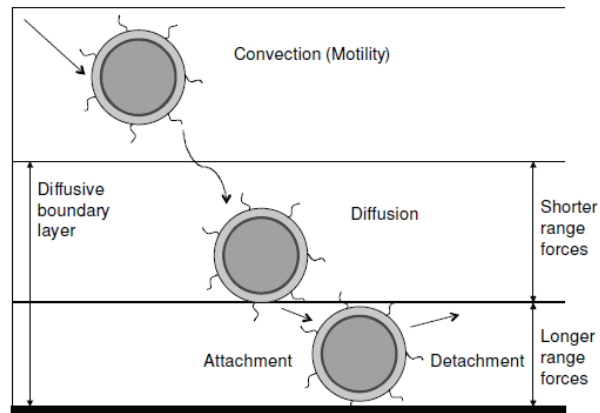


Figure 2.2: Attachment of bacteria cells mechanism by Dickinson[18]

## 2.2 Theory themes (DEP-EWOD)

In this part all physical theory is presented and explained. DEP is explained in two parts, what DEP force is and how results to be an important part in the manipulation of dielectric particle. EWOD is explained by its basic mechanism and applications. Both mechanisms were selected for repel bacteria from the surface.

**EP** Electrophoresis is the motion of particles by the appliance of an uniform Electric field.

**DEP** Dielectrophoresis is the manipulation force of polarisable (uncharged) dielectric particles by the use of non-uniform electric field.

**eDEP** electrode-less DEP due to a dielectric constriction of the electric field on a narrow space. Fig.2.3a

**TW DEP** Travelling wave DEP produces forces that pushes particles in/off the direction of wave propagation. (depending on the polarity of imaginary factor of CM) Fig2.3b

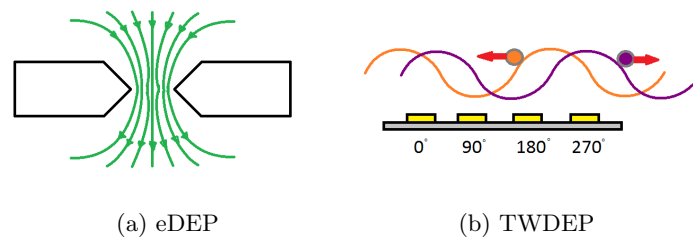


Figure 2.3: DEP variations

This last two are DEP variations that are considered in selected methods as a possible result in the tests purpose.

**EW** Electrowetting is the surface properties modification due to applied electric field.

**EWOD** electrowetting-on-dielectric is EW on top of dielectric-coated electrodes.



Considering the last shown methods and having a manufactured device composed of interdigitated gold electrodes covered with PTFE (dielectric layer, Teflon); these cases can be studied as part of applied voltage.

### 2.2.1 Dielectrophoresis Force

In this part Dielectric Force is explained, as well the Clausius-Mossotti (CM) factor.

Before explain of Dielectrophoresis, electrophoresis must be first defined.

Electrophoresis is the coulomb force created due to a electrostatic charged particle that moves (if it is DC potential) or stay still (if it is AC potential).

Electrophoretic mobility is described by Eq.2.1 and considering a “Thick double layer” is described by Eq.2.2

$$\mu_e = \frac{\vec{v}}{\vec{E}} = \frac{\varepsilon_m \varepsilon_o \zeta}{\eta} \quad (2.1)$$

where  $\varepsilon_m, \varepsilon_o$ , are medium and vacuum permittivity,  $\zeta$  is the zeta potential and  $\eta$  is the dynamic viscosity.

$$\mu_e = \frac{2 \varepsilon_r \varepsilon_o \zeta}{3 \eta} \quad (2.2)$$

Considering this and restricting it to dielectric particles, the study is focused on how electric field gradient affect the particle charge.

In order to define Dielectrophoresis (DEP), DEP force must be detailed as it is the main physical concept that influence this phenomenon.

The main force exerted by a gradient electric field in a general manner is described by Eq.2.3 where  $\varepsilon^*$  stands for complex permittivity.

The time-average force is:

$$\langle F_{DEP} \rangle = 2\pi r^3 \varepsilon_o \varepsilon_m \Re \left\{ \frac{\varepsilon_p^* - \varepsilon_m^*}{\varepsilon_p^* + 2\varepsilon_m^*} \right\} \nabla |\vec{E}_{rms}|^2 \quad (2.3)$$

where  $\varepsilon^*$  is the complex permittivity(vacuum, medium or particle),  $r$  is radius of the particle, and  $\vec{E}_{rms}$  is the electric field.

But considering spherical or cylindrical particles the equation can be reduced to Eq.2.4.

$$F_{DEP} = \frac{\pi r^2 l}{3} \varepsilon_o \varepsilon_m \Re \left\{ \frac{\varepsilon_p^* - \varepsilon_m^*}{\varepsilon_m^*} \right\} \nabla |\vec{E}|^2 \quad (2.4)$$

$$\varepsilon^* = \varepsilon + j \frac{\sigma}{\omega} \quad (2.5)$$

where  $l$  is the cylinder length,  $\varepsilon$  is the dielectric constant  $\sigma$  stands for conductivity and  $\omega$  is the frequency domain. Last but not least  $\Re\{f\}$  is the real part of Clausius-Mossotti(CM) factor  $\{f\}$ .

It can be concluded from above that the force magnitude depends strongly on the polarizability of the particle in respect of the medium. This motion of particles resulting in polarization forces by an gradient electric field was named dielectrophoresis by Herbert A. Pohl in 1950[19].

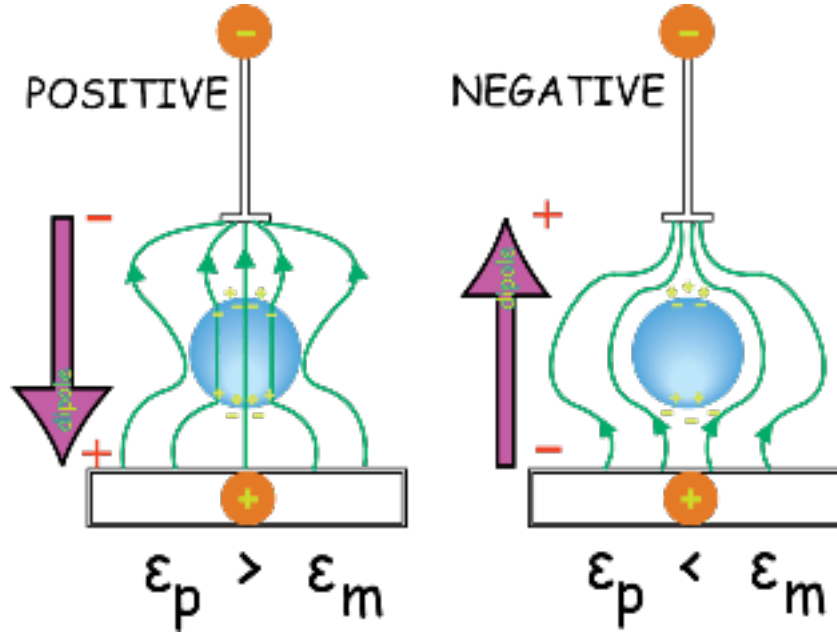


Figure 2.4: Movement of the particle under  $\vec{E}$

### 2.2.2 Dielectrophoresis in DC and AC Fields

In this part it is showed how DEP works in DC and AC fields. Finally they are compared for our purpose.

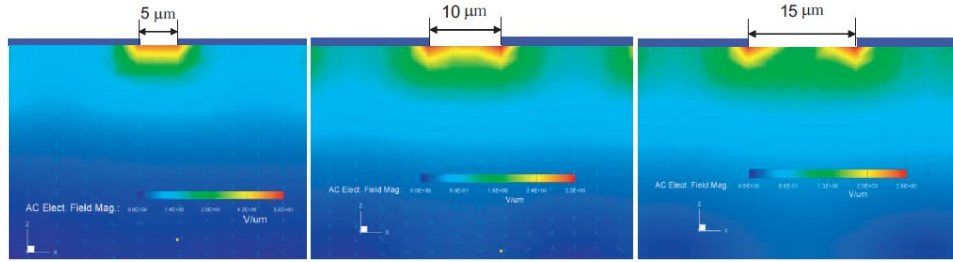
Consider the two cases:

**Non-uniform DC electric fields** the particle (now charged) will move along the electric field force. In the light of the particle dielectric property, if it is higher than the medium it will move towards the highest gradient field area (positive DEP (pDEP)) otherwise it will move towards the lowest gradient field area (negative DEP (nDEP)) as seen in Fig.2.4.

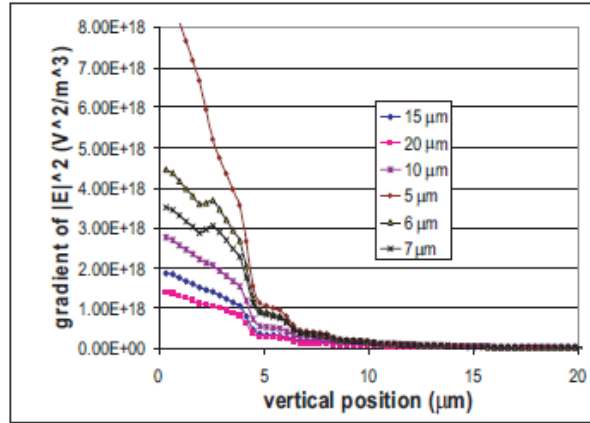
**Non-uniform AC electric fields** Aside from the charged particles (they presents little movements due to the exerted opposite forces produced by the AC field), depending on dielectric particles properties, it will follow the same behaviour of non-uniform DC. As a consequence, positive DEP ( $\Re\{CM\} > 0$ ) and negative DEP ( $\Re\{CM\} < 0$ ) will work as trapping and rejecting particle method respectively.

From above cases, it can be seen that DEP force depends strongly on  $\vec{E}$  gradient. By reckoned to it, this information can be deduced:

- $F_{DEP}$  is proportional to particle volume and  $\varepsilon_m$ . Its direction is within  $\nabla|\vec{E}|$  rather than  $\vec{E}$ .
- $F_{DEP}$  is inversely proportional to the cube of the electrode distance (gap). As seen on Fig.2.5.



(a) Electric field on 5, 10 and 15 μmgaps



(b) Electric field gradient vs. gap distance

Figure 2.5: Interdigitated electrode distance effect on Electric field[1]

### 2.2.3 EWOD in DC and AC fields

In this part EWOD is similarly presented and compared not only by DC and AC fields but the difference in frequency values.

To this extent, DC voltage is applied to see how the contact angle change as part of the force created by the electric field and how that force overcome the surface tension (Gibbs free energy) while the potential increases between the electrodes and the medium (capacitance).

By applying AC voltage the result is the same but depending strongly on the frequency applied the contact angle changes and return to its original position (zero potential) in a dynamical speed.

The electrowetting principle reckon on the described Lippmann-Young equation Eq.2.6

$$\cos \theta = \cos \theta_o + \frac{1}{2} \frac{C}{\gamma_{LG}} V^2 \quad (2.6)$$

where  $\theta_o$  is original contact angle (without electric field),  $\theta$  is the one with the electric field,  $C$  is capacitance per unit area (between electrodes and liquid),  $\gamma_{LG}$  is the surface tension vector (liquid-gas) and  $V$  is the applied voltage. It must be considered: de-ionized water  $\gamma_{LG} = 30 \text{ mN/m}$ .

### 2.2.4 Theory limitations

In this section limitations are displayed and justified, including: the Debye layer, the ion diffusion on Electrical Double-Layer (EDL) as seen on Section 2.1, REDOX on electrolysis and joule-heating as part of the inherently happening in the proposed microenvironment.

It is important to consider also the limitations presented in every experiment in regard of the theory presented.

- $F_{DEP}$  is proportional to square of voltage. (reversing BIAS does not reverse force)
- Joule heating effect can be neglected as the resistance and low voltage can reduce the electrical current considerable in this stationary test.
- As long as the Debye layer is able to be present in ionic medium, it must be taken on count but can be neglected if the force is high enough compared to EDL.
- Other limitations not accounted for like taking as constant values for dielectric, permittivity, conductivity, viscosity, resistivity, and more inherent properties of the particle, medium and surface materials.

## 2.3 Modelling of biological cells

In this part Biological particles are modelled in a layered approximation, also is presented the effect of a hydrophobic dielectric for EWOD applications.

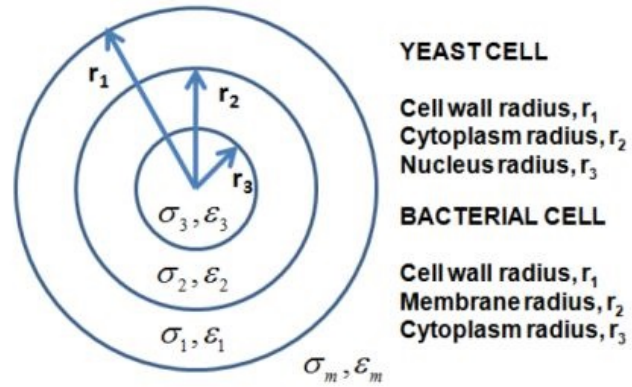
The bacteria that was used is *Salmonella typhimurium*, which is characterized for having cylindrical surface and a tail.

### 2.3.1 Biological cells on DEP

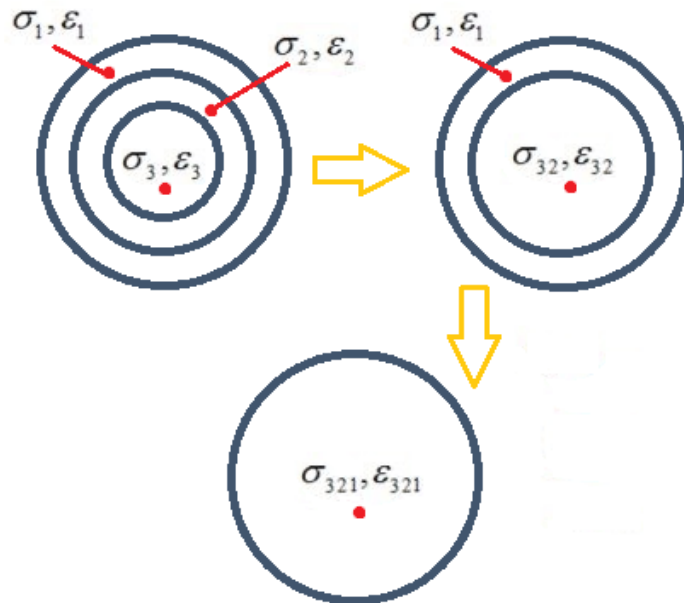
In this part it is illustrated the approximation modelling of bacteria cell as a three concentric layer particle and details of calculation of the complex permittivity needed to calculate the CM factor.

As bacteria is not a single particle but a particle made of different conductivity layer; it has been modelled as followed in Fig. 2.6a where bacteria is studied as an spherical shell model.

**DEP model of a biological cell as a particle with three concentric layers**



(a) DEP multi-shelled cell modelling



(b) Spheric approximation of multi-shelled particles by smeared-out sphere approach

Figure 2.6: DEP cell modelling[2]

From Fig.2.6a can be seen that having the conductivity and permittivity data the right frequency can be calculated.

But considering a wider range frequency where bacteria change its CM factor DEP can be used.

### 2.3.2 Hydrophobic effect on bacteria adhesion

In this part is presented a study of how surface energy is directly translated into hydrophobicity, and how adhesion works on that.

Bacteria adhesion is measured in free energy of interaction ( $\Delta G_{iwi}$ ). And so it is the hydrophobicity measurement, where if  $\Delta G_{iwi} > 0$  it is hydrophilic, and if  $\Delta G_{iwi} < 0$  it is hydrophobic.

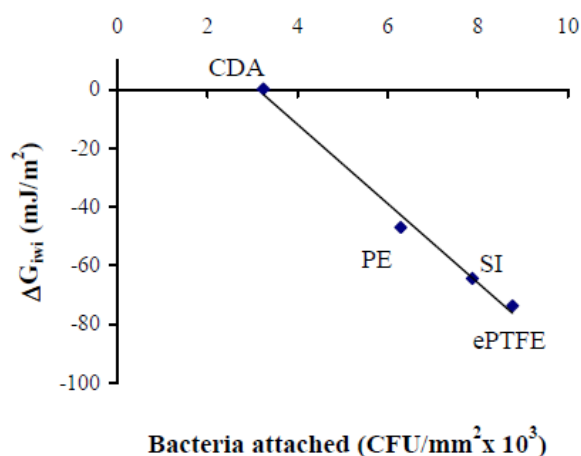


Figure 2.7: Relation between the number of attached cells of *Staphylococcus epidermidis* ATCC 35984 (RP62A) and the degree of hydrophobicity ( $\Delta G_{iwi}$ ) of various types of substrata,ref [20]

From the Figure2.7 it can be seen how linear is the relationship between both measurements, confirming by this way how hydrophobic bacteria are interact easier with hydrophobic surfaces and same with the hydrophilic interactions.

## 2.4 Modelling of electrodes

In this part electrodes configuration is selected by its purpose and an electrical modelling is approximated according to the material electrical values.

After seen the theory and limitations presented for this phenomenon, the next step is to select the best electrodes array for the Project goal.

There are several electrode configurations studied and applied in dependence of the operating strategy.Fig2.8

The selection of the electrodes array, in the electrode pattern, is interdigitated beneficial to levitating the particles in DEP and making the particles flow over them without reaching the bottom.

By having an open EWOD design, with interdigitated electrodes, rejecting bacteria can be possible.Fig.2.9

From here having a DC square signal, changing from positive to negative in one period, allow bacteria to stand still in a Electrophoresis manner, while the electric field is constant at all time.

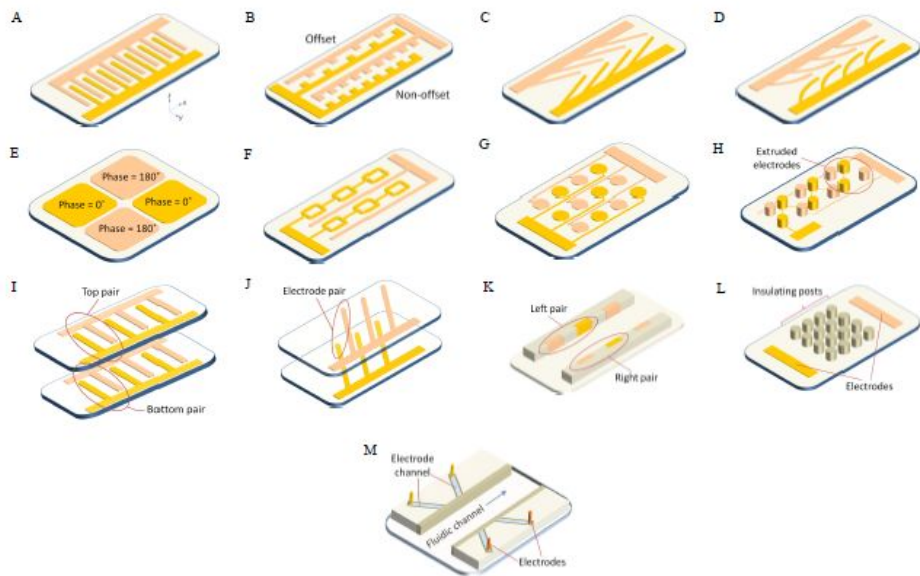
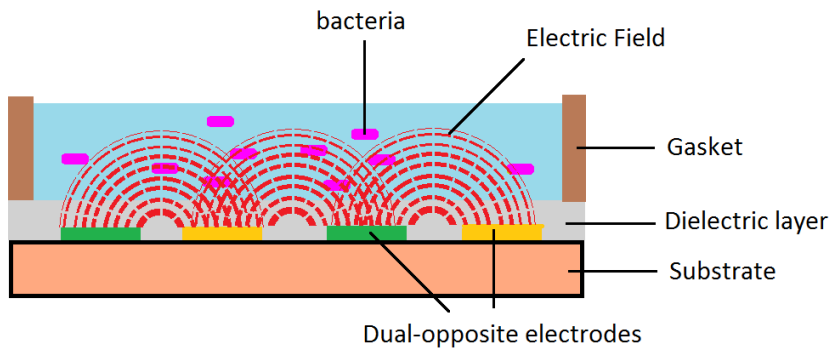
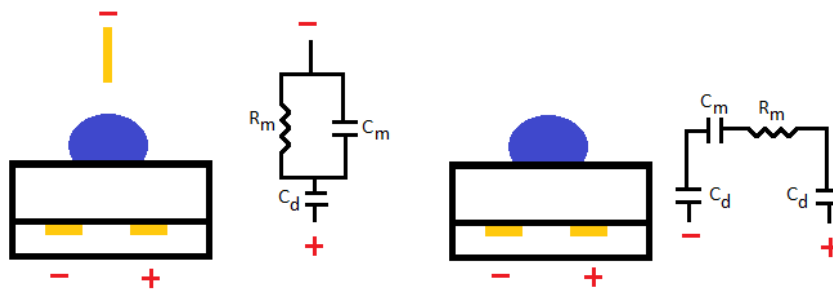


Figure 2.8: Classification of DEP devices according to the configuration of microelectrodes: (A) parallel or interdigitated, (B) castellated, (C) oblique, (D) curved, (E) quadrupole, (F) microwell, (G) matrix, (H) extruded, (I, J) top-bottom patterned, (K) side-wall patterned, (L) insulator-based or electrodeless, and (M) contactless,[21]



(a) EW electric fields affecting bacteria



(b) Electric Modelling of the setup

Figure 2.9: EW electric fields and equivalent Electric circuit

## Chapter 3

# Design and assembly of the experimental setup

This part describes the wafer fabrication which consist of the assembly of the electrodes array onto a glass surface using standard MEMS technology processes.

Several aspects of the design had to be considered in order to adapt the experimental device to the measurement setup available; transparent substrate and thin device layer for observation of the bacteria through an inverted fluorescent microscope, oil based lenses, culture time, and Teflon layer deposition.

The design and assembly can be summarized to 3 stages: electrodes design, chip fabrication and gasket moulding. *The electrodes design* was started on L-Edit® program, where the interdigitated electrodes arrangement resulted to be the most suitable for the DEP rejecting bacteria application as it is explained later on. *The chip fabrication* was done in the clean room in KTH Kista facilities because of the micro scale proportions of the electrodes design; metal sputtering, lithography, etching, dicing and finally Teflon spinning were done to build the final desired chip.

Finally, it is shown how *gasket design and fabrication* were made for containing bacteria on top of the produced electrodes.

### 3.1 Chip design and assembly

This part describes the chip manufacturing by designing the electrodes and then metal sputtering, photo-lithography, etching and dicing needed to obtain the wafer with gold electrodes on top of it. Finally a Teflon layer is spun which makes possible to act as an capacitor for EWOD tests purposes.

#### 3.1.1 Electrode design

fitting it on a round wafer shape presented a big challenge. Detailed pictures of the wafer design are depicted.

The investigated electrode design of interdigitated electrodes was chosen because it was the most suitable and flexible design for DEP and EWOD applications according to the Fig.2.8[21]



as it was shown in Section 2.4.

In this case a wire-free configuration[22] on top of a glass substrate of golden interdigitated electrodes is presented, in contrast to the conventional EWOD configurations as it can be seen in Figure 3.1a.

The L-Edit software is used to design the electrodes layout, which have been planned to have 3 different widths (a, b in Table 3.1) keeping the length of each electrode constant ( $l=6.450\text{mm}$ ) as seen in Fig 3.1b. The a and b variables were chosen within the bacteria scale size ( $<10\mu\text{m}$ ).

|        | 'a' $\mu\text{m}$ | 'b' $\mu\text{m}$ |
|--------|-------------------|-------------------|
| Case 1 | 5                 | 10                |
| Case 2 | 10                | 20                |
| Case 3 | 20                | 50                |

Table 3.1: Different width of the electrode depending on the case used

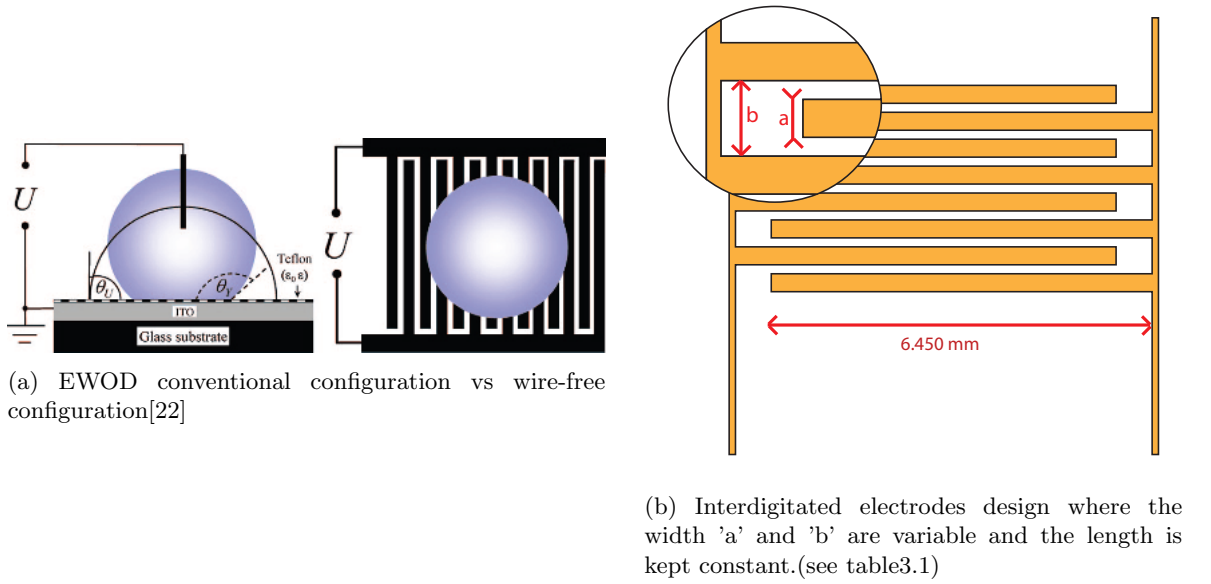


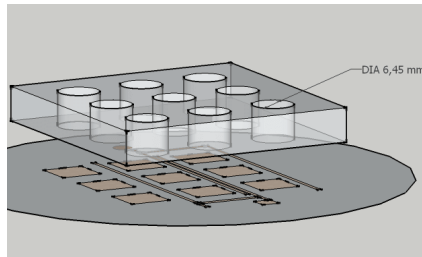
Figure 3.1: Electrodes configuration

From the diameter of the gasket holes that is used for contain bacteria medium, the electrode design length is defined by the gasket holes diameters. That should stand on top of each square regions (as seen on Fig.3.2b) where the electrodes are as it can be seen in Fig.3.2a. From this squares, 6 are active and the last 3 are left to negative control (no power supply is applied by not connecting to the power grid).

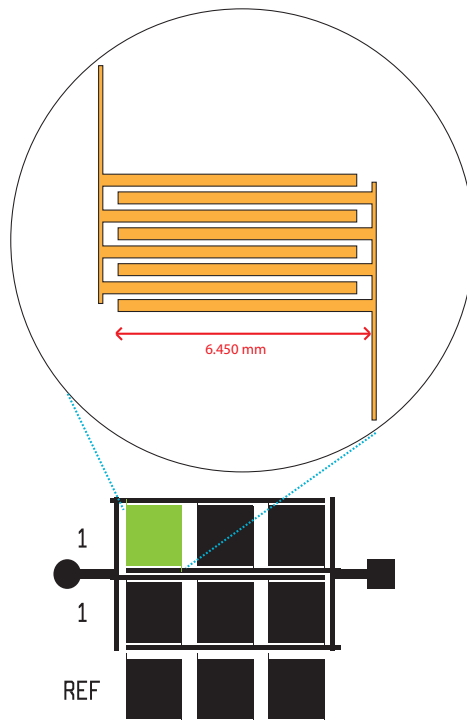
Arranging four of these tests areas (chips) can fit on one single wafer as it can be seen in Fig.3.3b. In addition, each chip has been numbered with case 1, 2 or 3 as used in Table 3.1 to difference each chips at the experimental part, this is seen in Fig.3.3a. From this is seen case 1 was repeated twice on each wafer to be considered more relevant because DEP forces act stronger within smaller scale environments as it was explained in Subsection.2.2.2.

### 3.1 Chip design and assembly

---



(a) Gasket on chip to see the electrodes length reason



(b) Interdigitated electrodes spaced on a quarter of a 10 cm diameter wafer.

Figure 3.2: Electrodes in square spaces

#### 3.1.2 Chip fabrication

The following subsection describes the process and details involved in the manufacture of the wafer, from the layer structures that are planned from the beginning until the Teflon spinning of the final finished wafer passing through the lithography, etching of the metal electrodes and dicing of the complete wafer. All procedures of this fabrication were done on Kista Campus at KTH facilities.

The procedure is outlined below:

1. *Glass wafer*: 500 $\mu$ m of thickness

### 3 Design and assembly of the experimental setup

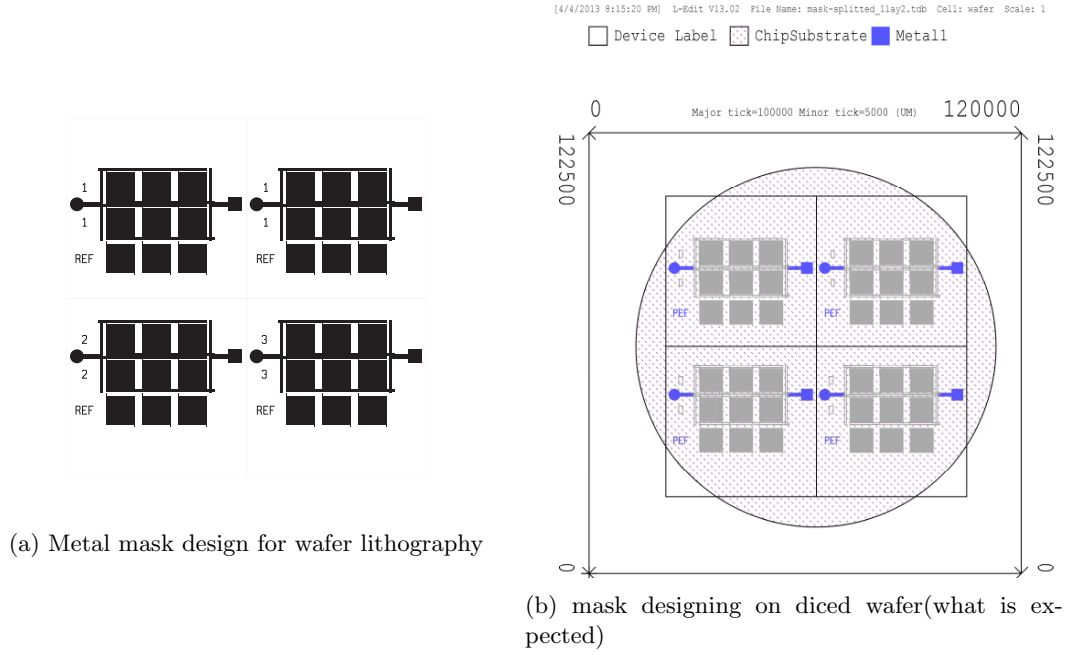


Figure 3.3: Mask and expectable wafer design

2. *Sputtering Metal*: TiW (200Å) under Au (1500Å) layer
3. *PhotoResist(PR)*: Type nLOF2070 is used
4. *Development*: three minutes of duration
5. *Etching*: First layer (Au)
6. *Etching*: Second layer (TiW)
7. *Striping*: Last layer (PR)

#### Process

The different deposited layers are shown in Fig3.4. In this part is shown the Metal deposition in a structural order (layers) for a better understand of the final display.

#### Metal Deposition

The metal deposition was made in a metal sputtering machine (KDF® 844NT, Model 844GT), using DC sputtering system. It was needed to sputter the Titanium Tungsten alloy (TiW) in the glass wafer to make the adhesion of the gold stronger to the wafer surface. It was sputtered 20nm of that alloy, and on top of it 150 nm of gold metal.

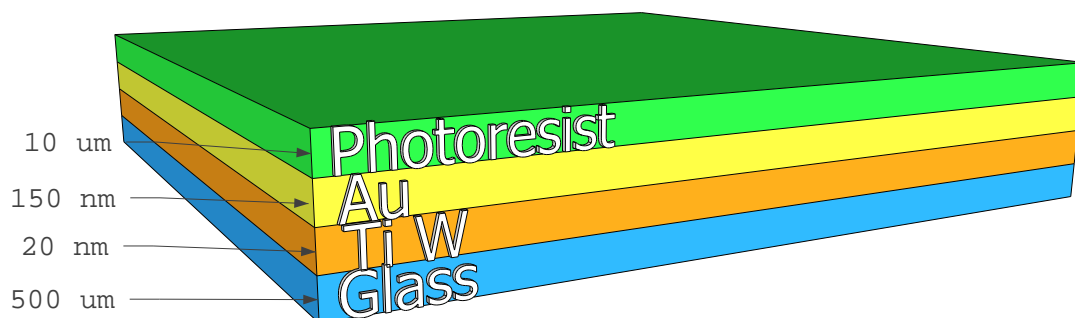


Figure 3.4: Different material layers that constitute the final Wafer Structure

### Structuring of gold

**Lithography** In this part is detailed the photo-lithography used, photoresist and time setup is also included finished with the respective development for a finest finish.

To define an etch mask for the gold, a photoresist layer (PR film) is spun on the wafer, AZnLOF2035 RER 600 (2:1), in a OPTI®spin machine model SST20(SSE) at 3000 RPM for 30 s with a final soft bake at 90° C for 60s.

The photo-lithography intended to be applied by the earlier design metal mask Fig. 3.3a is useless if the application of the PhotoResist (PR) is not coated carefully. For coating the samples is used as PR film.

Next, the Ultraviolet(UV) light (UV) exposure dose was optimized through some tests to reach the ideal exposure parameters (Table3.2) and used on a Karl Suss®, MA6/BA6KSM model machine with the metal mask (Fig.3.3a).

|  | Lamp intensity         | Lamp power | Wavelength |
|--|------------------------|------------|------------|
| Mode CP<br>with 10 s of Lo Vac Contact<br>and Alignment Gap of 40 μm | 18,3 $\frac{mW}{cm^2}$ | 350 W      | 450 nm     |

Table 3.2: Photoresist curing time parameters

Lastly, to finish the Lithography process is required its development. After baking on a hot

plate to cross-link the PR, the wafer is *developed for 5:05 min (included post baking)* to remove the unexposed areas of PR film. This process is automatically executed by MAXIMUS® machine.

Photo-lithography is process is explained in Fig.3.5

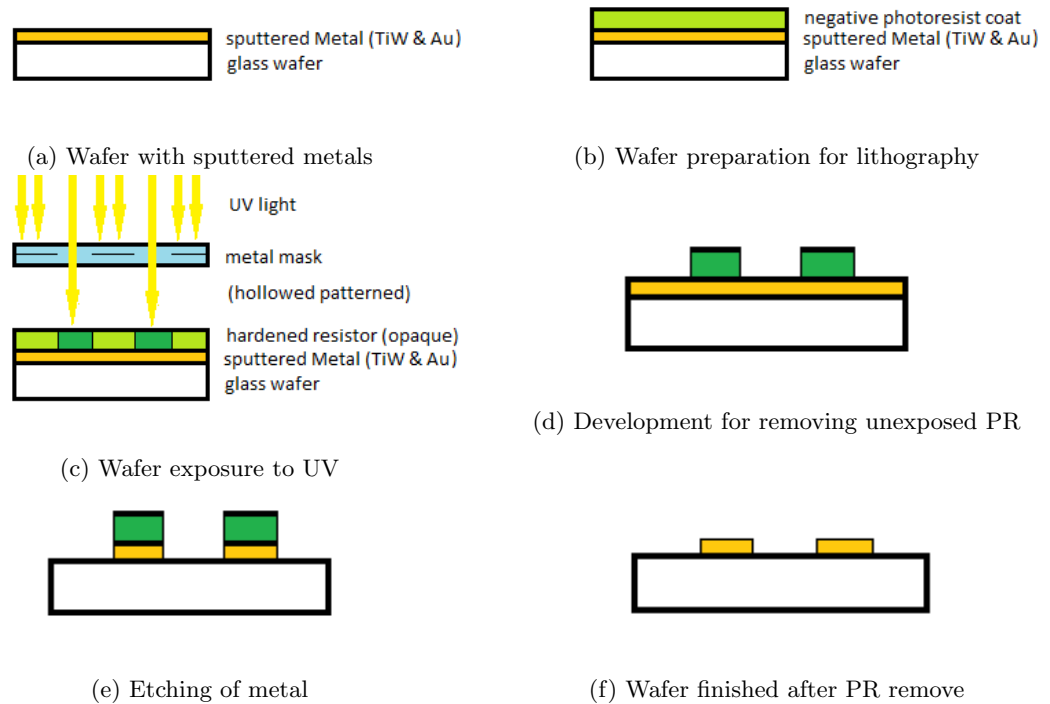


Figure 3.5: Process of Photo-lithography

**Etching** Etching consists in the removal of unwanted metal layers from the glass surface, such as sputtered metal that does not belongs to the electrode pattern.

In this part each metal etching is detailed with their respective recipe formula where having many different electrodes widths made this a complex task resulting in some over etching or poor etch finishing.

As the layer of gold is the first one from the top, it is wise to start with it.

Au ETCH FORMULA:

- 60 g of  $I_2$
- 240 g KI
- 2400 g  $H_2O$

On proportion (1:4:40): etch rate 5,8 nm/s.

Considering our electrodes having different width, different times were used with the aim of etching the more quantity of metal without affecting the design amplitude of the electrode.

### 3.1 Chip design and assembly

---

#### Au ETCHING METHOD:

For every glass wafer 30 s at 10 RPM where etched in the whole wafer area. Additively, an extra time was tried according to the following Table3.3 in manual mode(static).

|           | #1  | #2 & #3 |
|-----------|-----|---------|
| 1st wafer | –   | –       |
| 2nd wafer | 5 s | –       |
| 3rd wafer | 5 s | 3 s     |

Table 3.3: Different used etching times on lithography

In the same way the TiW layer is etched.

#### TiW ETCH FORMULA:

- 31% 50  $H_2O_2$  @50° C: etch rate 1.25 nm/s.

#### TiW ETCHING METHOD:

The etching liquid is poured manually onto the glass wafer during 20 s. This process is refined by feedback from the laboratory microscope.

In this way, time can be measured and see how far the etching can go without over etching the electrodes.

**Dicing** In this part it is explained how glass wafer is diced and the parameters used for the saw machine setup in order to extract the chips from the finished etched wafer.

Finally, dicing of the wafer depending on their material (glass or Silicon, as seen on Table.3.4) is crucial as the machine parameters counts on it. In this case, the Dice Saw used was DISCO<sup>TM</sup> DAD 320.

|               | Spindle speed | Feed Speed |
|---------------|---------------|------------|
| Glass         | 14'000 RPM    | 1          |
| Silicon oxide | 30'000 RPM    | 5-10       |

Table 3.4: Spindle and Feed speeds for the different materials

It is important to consider which parameters to enter into the dicing machine; there are a lot of parameters depending on the kind of wafer and size of them, but changing of some of this parameters must be done with the purpose of achieve the most accurate dice of the wafer.

The parameters used on this process are filled on the tables Table3.5 and Table3.6.

**Teflon layer** In this part is described how Teflon layer is formed, and the thickness of it. Considering the wafer electrodes shapes an insulating technique is also added.

Teflon  $(C_2F_4)_n$  is formed with the mix of 0.6 % Teflon and FC-40 in a dilution ratio of  $1/7$ .

Depending on the desired thickness of the layer, the spinning speed and acceleration is also set it up. The spin coater used was SPIN 150– NPP. In order to have 480 nm of *thickness* in our samples, a 1200 RPM speed is selected within 60 s at 100 RPM/s of acceleration.

### 3 Design and assembly of the experimental setup

---

| P1A851             | Work thickness (wafer thickness) | Blade height | Tape thickness (blue tape) | Rnd(round work size) | z-axis down speed |
|--------------------|----------------------------------|--------------|----------------------------|----------------------|-------------------|
| Machine Parameters | 0,8 mm                           | 0,0650 mm    | 0,05 mm                    | 110 mm               | 10 mm/s           |

Table 3.5: Glass Blade parameters

| ZH05-SD2000-N1-70 EE | Work thickness (wafer thickness) | Blade height | Tape thickness (blue tape) | Rnd(round work size) | z-axis down speed |
|----------------------|----------------------------------|--------------|----------------------------|----------------------|-------------------|
| Machine Parameters   | 0,55 mm                          | 0,1 mm       | 0,08 mm                    | 120 mm               | 10 mm/s           |

Table 3.6: Silicon Oxide Blade parameters

Subsequently, the chip is heat it up on a two-steps procedure in a hot plate, at 165°C for 10 min and then 200°C for 25 min. The hot plate used was IKA® C- MAG H57. It is important to keep it an eye on it at all time, and in an vacuum chamber because Teflon vapours are very dangerous. Thereafter keep the sample cold down for 20 min.

With the intention of keep Teflon only in the electrode's area, a high temperature film was used, and carefully stuck to the chip. But this only worked on glass substrate rather than in the silicon glass substrates as it is illustrated in Fig.3.6

**Finishing** In this part the finished wafer is presented and the next steps are described like repairing not well etched electrodes and soldering the copper wires.

At the end of the chip fabrication it is important to reassure that the design measurements have been achieved or at least are near to them.

First, the metal mask is measured(Fig.3.3a). Particular measurements can be seen on Fig.3.7.

Finally the wafer is ready to be prepared Teflon covering as it can be seen on Fig.3.8

**Comments** Concerning the wafer fabrication process, some problems arose from the design to the etching part.

For the setting of the electrodes array design, the approach was to mimic the 96- wells plate that are used in biological laboratories (Fig.3.12a as it is going to be explained in Section3.2), which could not be done because considering the material and standard space employed by the culture plates is big but cheap; the cost to achieve this in a wafer fabrication (Fig.F.2) can be very high and also ineffective counting the error samples that can be made in the etching process (as it did with the new design).

During the etching, the major challenge was equilibrate the periods of time defined for the smallest electrodes and the bigger ones.

For example, it was needed more time for the smallest ones (Case1) so over-etching were seen (red shrinking arrows in Fig.3.10); while for the bigger electrodes (Case 2 and 3), the required time was less and it resulted in under-etching of the smallest electrodes (green increasing arrows in Fig.3.10).

About the finished wafers, it has been found that due to the different size gaps in the electrodes, the etching times for each electrodes case were different. This become on a major problem to over etch some electrodes (the smallest ones) or under etch others (the biggest ones). In the smallest ones, was very common to see traces of gold etched particles, which close the circuits by touch to consequent electrodes.

### 3.1 Chip design and assembly

---

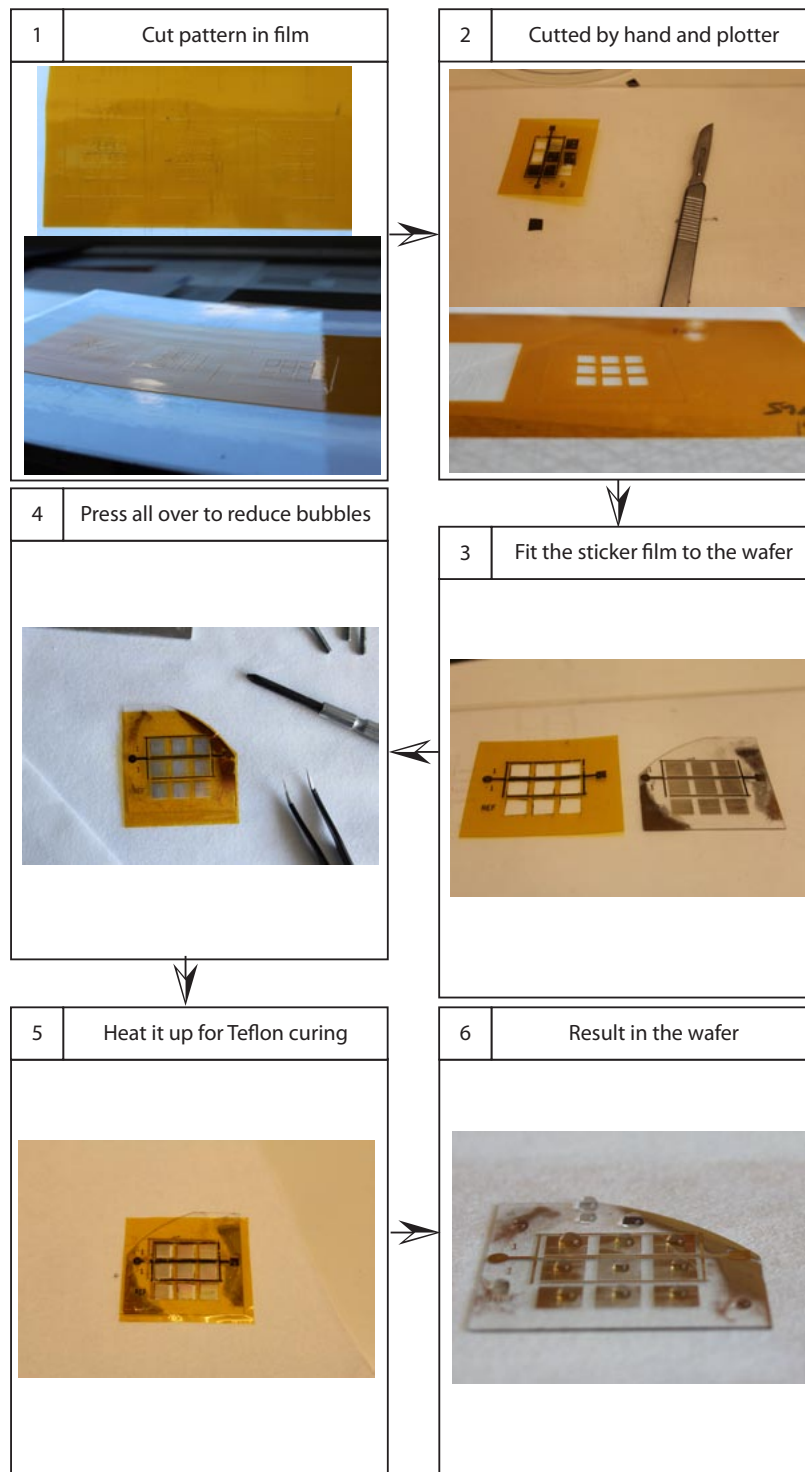


Figure 3.6: Teflon technique to insulate on only electrodes



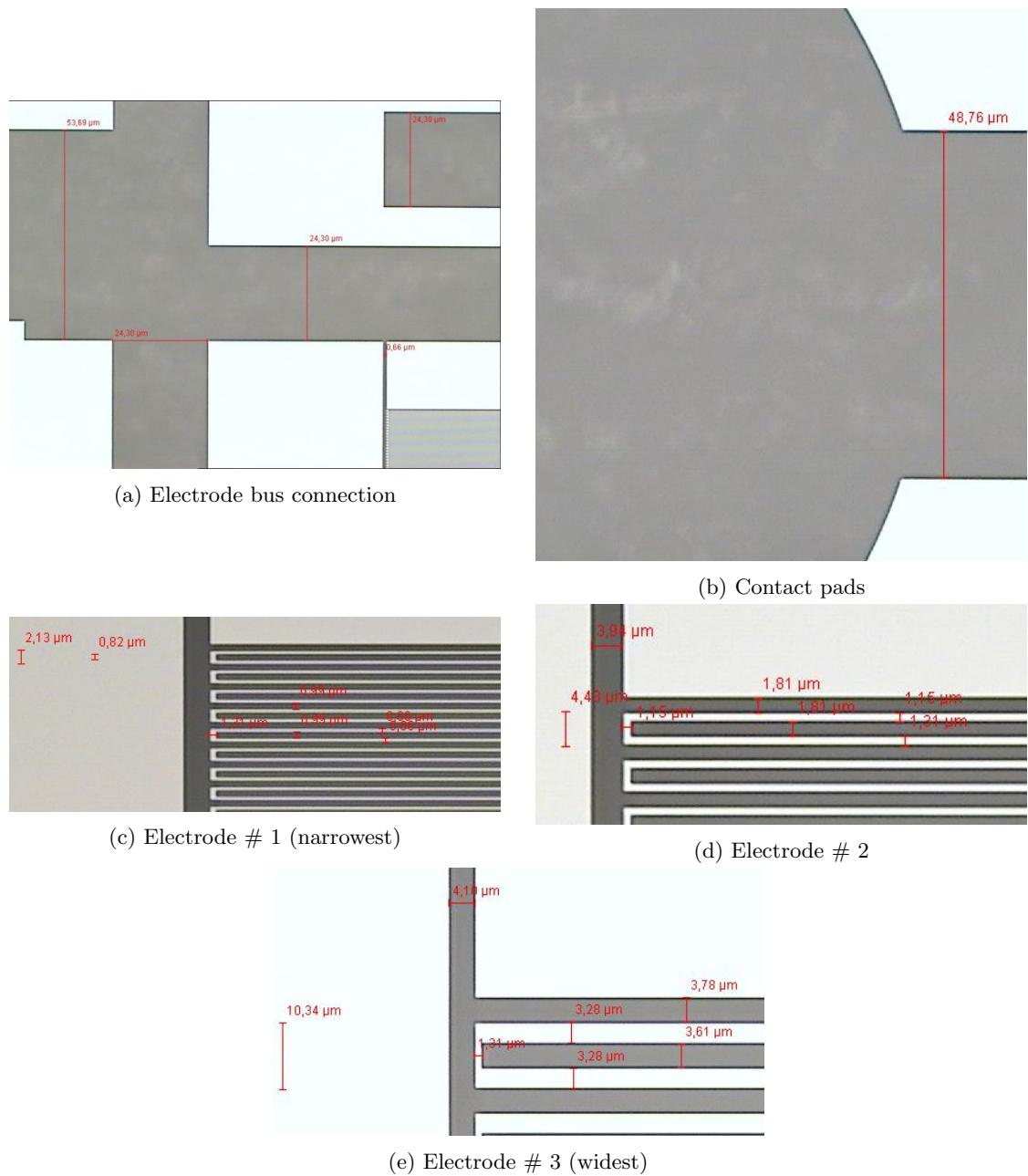


Figure 3.7: Metal Mask Measurements

This problem was solved opening the short-circuited electrodes with a sharp diamond needle (same used for cutting the glass slides for the gasket moulding).

Next, the main concern in Teflon spinning was to achieve a thicker layer enough to act as a capacitor but thin enough to allow electric field to act on particles by EWOD. Several iterations of spinning time and curing temperature were done to achieve the final height ( $\sim 500$  nm).

Some of the key problems were the way Teflon was uniformly spanned on the spinning

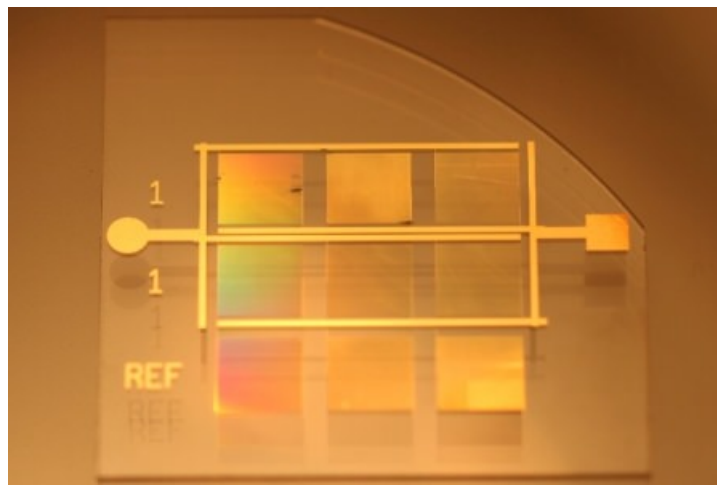


Figure 3.8: Diced finished wafer

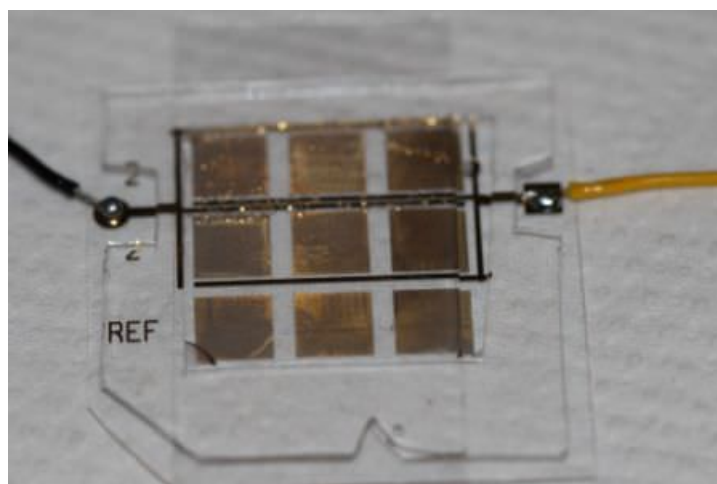


Figure 3.9: Final built test device

machine. If there were any particle or bulk on top of the surface, it got affected making some sections covered by Teflon in a thinner level.

It has been found that using 2.25% of dielectric layer (Teflon) is too thin that breakthrough becomes easy to happen.

Finally the wafer is covered with Teflon and soldered to copper electrodes as it can be seen on Fig.3.9

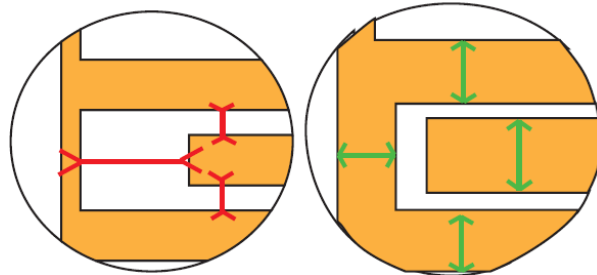
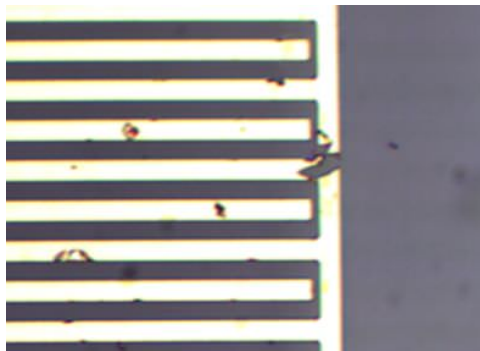
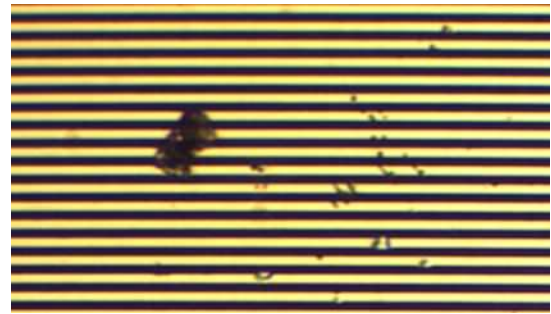


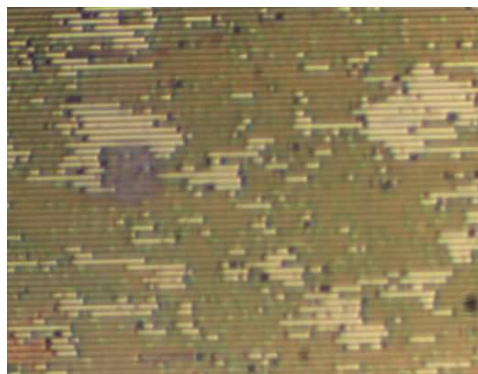
Figure 3.10: Etching time problem between Case 1 electrodes and Case 2 electrodes



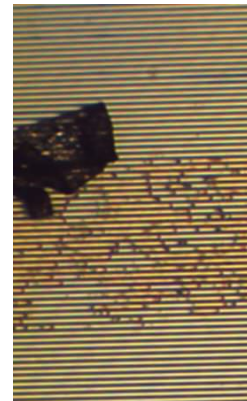
(a) Broken electrode bus



(b) Photoresist residue



(c) Photoresist and non-etched spots



(d) Irregular patterns over electrodes

Figure 3.11: Electrode bad etching finish

## 3.2 Gasket fabrication

In this section a gasket design is developed in order to contain the bacteria medium on top of our chip (manufactured diced wafer glass). Two materials are analysed to be used as a gasket for the bacterial medium container.

Two versions were fabricated, the first one made with off-stoichiometry thiolene (OSTE) was first attempted to be a single gasket with 9 holes on it, planned to be over each respective electrodes cells of the chip; as a second attempt and to get the perfect curing time for the gasket material a single hole well tests were made. The latter one, was made of PDMS for the sake of practicality and rapid careless fabrication, by this a simple big hole was used in this case.

The main design limitations presented were the thickness (knowing how much medium was going to be enough for the experiments), size (covering all the chip but not over the edges to prevent leaking), easy detachment(keeping in mind that matching the right spot of attachment was not easy task)and evaporation of the medium during the time without affecting the observation procedures.

### 3.2.1 Gasket version 1

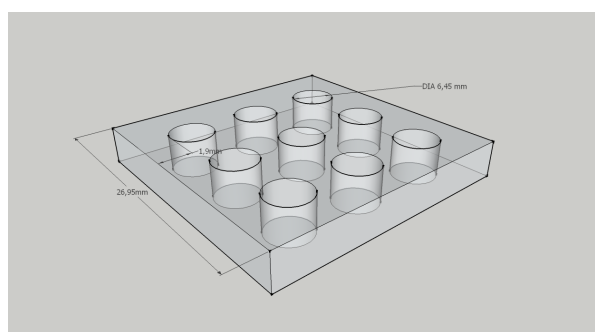
In this part OSTE, a novel polymer platform based on off-stoichiometry material[23], is selected for its flexible properties as a new product for this purpose. This was made mainly for the tuning abilities of the material and its versatility for complex moulding.

In view of emulating the well (Micro-titre) plates that are used by the bacterial tests, first attempts and later single well are made.

The chip was made based on the size of the wells from the Cell Culture Plate (96 Well) Sterilin®, which its wells diameter  $\phi$  is constant ( $\phi = 6,45\text{mm}$ ) as it can be seen in Fig3.12a. By the same way the gasket, was supposed to have the same characteristics of the mentioned Sterilin wells.



(a) Commercial Cell Culture Plate (96 Well) Sterilin®



(b) Design of the gasket to be done

Figure 3.12: Commercial gasket and design

The only elements used for the formulation were two types of monomers, a thiol functional group and an allyl functional group; combining together form the stoichiometric thiol-ene network polymer, but for making OSTE polymer only an excess of either thiol or allyl is done.

### First attempts

**Formulation, mixing procedure, UV curing** In this section the design is sought to fit into the well plate structure but is modified for better clamping and good sealing.

The OSTE formulation is based on 100 % thiol excess and can be seen on Table 3.7.

| Off stoichiometry | Thiol        | Allyl     | TPO-L(initiator) |
|-------------------|--------------|-----------|------------------|
| 50%               | PETMA 1.125x | TATATO 1x | 0.5 wt%          |
|                   | PETMP 1.125x | TATATO 1x | 0.5 wt%          |
| 80%               | PETMA 1.35x  | TATATO 1x | 0.5 wt%          |
|                   | PETMP 1.35x  | TATATO 1x | 0.5 wt%          |

Table 3.7: OSTE Formulation: Stoichiometry, monomers and curing agent

Once the right amount of monomers and initiator is selected, a pre-polymer mixing is required. In this case a vortex was used to have more homogeneous results; one of the major problems of using this is the presence of bubbles at the end of the mixing, which can be solved by introducing the sample on the vacuum for at least 30 min at a pressure of approximately -72 kPa.

Additionally the least quantity of light must be avoided from the sample just before the curing process. In order to cure the pre-polymer, UV curing (unfiltered) on OAI® UV curing lamp, is used to trigger the allyl reaction while the TPO-L for the respective thiol-ene.

**Preparation – aluminium moulds** In this part the aluminium moulds used for the shaping is illustrated in Fig.3.13 taking in consideration the size of the wells and a top-covering lithography.

Although the gasket results on some leaking and non-uniform surface due to the unknown exact UV curing time, single hole well tests were made.

### 3.2 Gasket fabrication

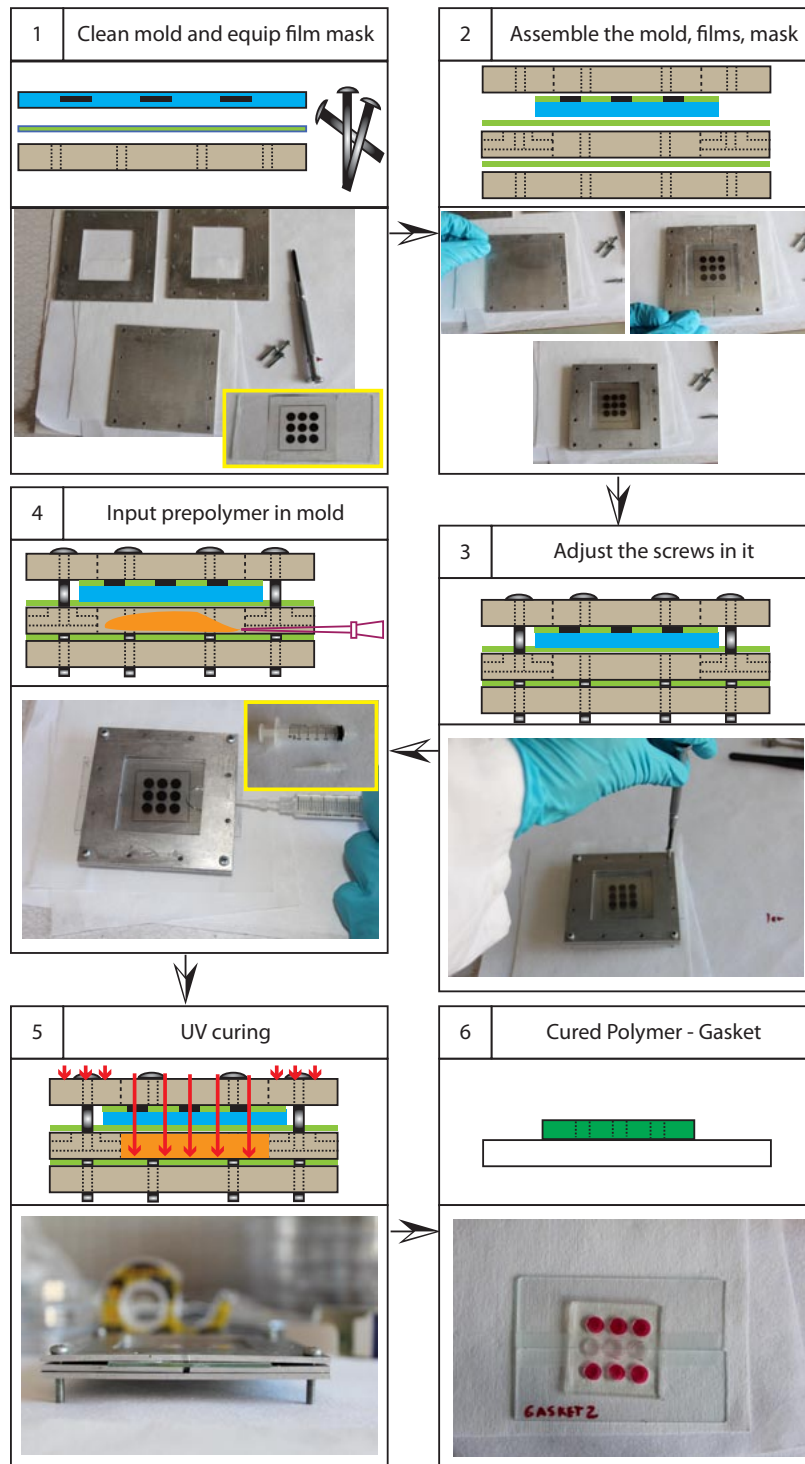


Figure 3.13: OSTE gasket on aluminium mould

### Single hole well tests

In this section it is detailed the process of preparation of single wells after first attempts were difficult to manage. Consequently to minimize the errors are, single hole wells were tested and their different thickness to finally prepare the desired design.

With the intention of calculate the exact amount of UV-curing time, tests were made by reducing the layer thickness and also making only one hole for practical measurements, from 5 mm to 2mm and 1mm respectively(Fig.3.14).The sealing tests were shown in Subsection 3.2.3.

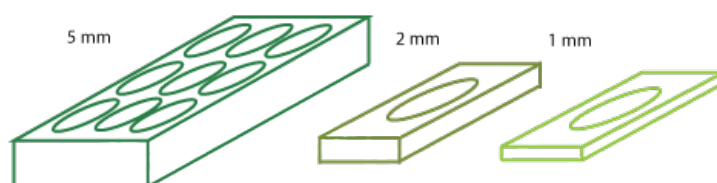


Figure 3.14: OSTE gasket and one hole gaskets designs

**Formulation, mixing procedure, UV curing** Here is described the formulation that is deduced from the first attempts section taking on count the finest shapes and transparency.

The formulation is the same one as the Table3.7. Despite the fact of using much less quantity of pre-polymer, consequently less UV curing time (less than 10 seconds)

**Preparation – glass moulds** In this case, aluminium mould were not needed as a result of not having big samples and trying only a little piece of polymer. Thus suitable glass slides were used to cleanliness and practicality.

In order to made a single hole, a very simple and quick mould should be used. By this, some glass slides were cut with a diamond burr type Flamme, from the Hobby Drill 2000 brand,as it can be seen in section 1 of Fig.3.15.

Once many 2cm x 2cm are cut, are glued with double side Scotch 3M® tape to a single glass slide which was previously covered with a Xerox® film.(to detach easily after curing).

Soon after, pre-polymer is poured on the glass mould and covered with the one hole film mask stuck to a glass slide. To prevent any leaking 2 clamps are fixed on the sides, and then inserted on the UV light chamber for the time is required.



### 3.2 Gasket fabrication

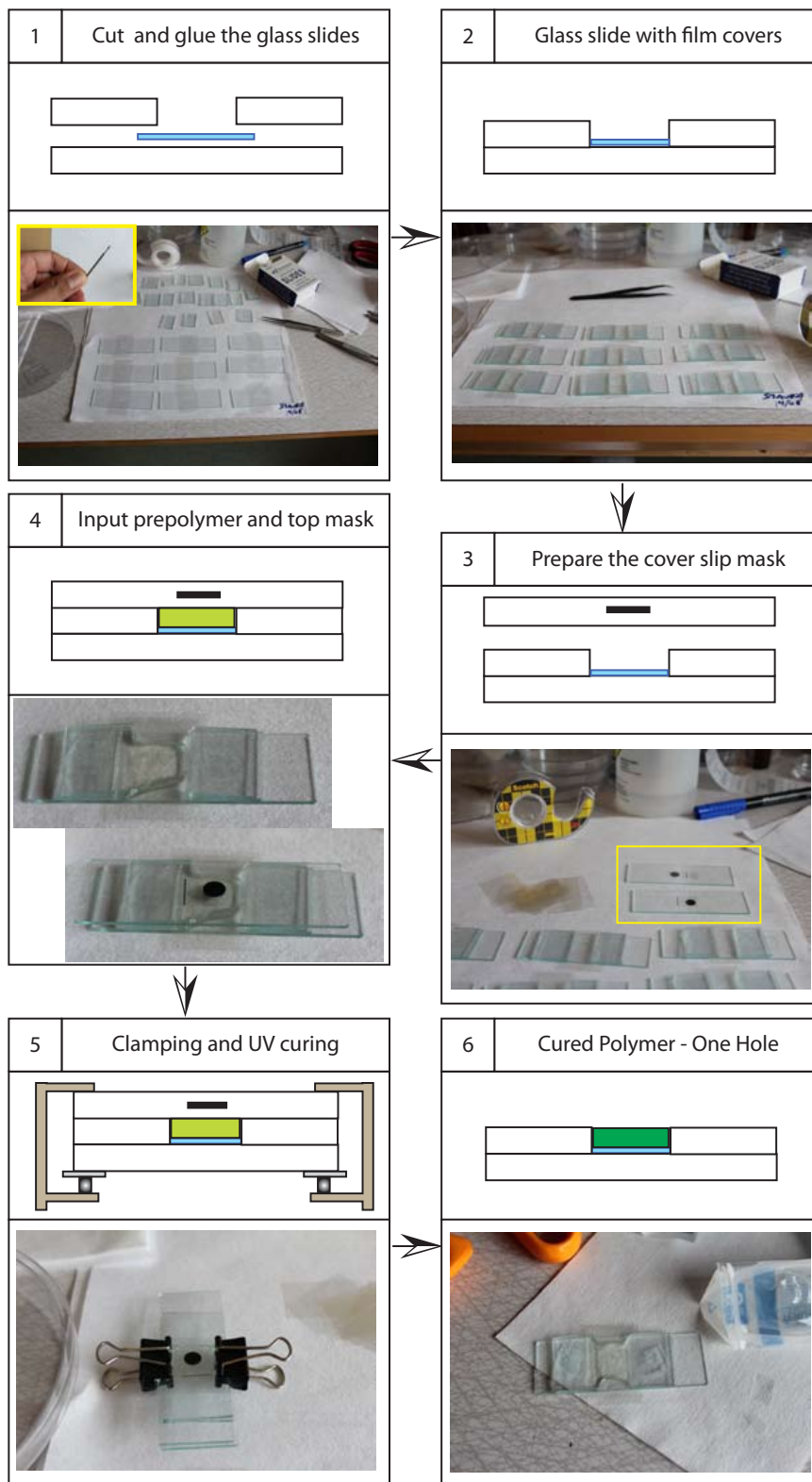


Figure 3.15: OSTE one hole gasket on glass slide mould



### 3.2.2 Gasket version 2

In this section a rubbery gasket(PDMS) is selected for a fastest way to manufacture and for stickiness to Teflon layer without the use of nine-hole gasket but a simple squared gasket. Moreover, process and moulding is detailed which a single big well was used.

PDMS known as well as dimethicone(Polydimethylsiloxane), is an organic polymer widely used. It was chosen due to its simple formulation and not UV-curing time dependent; of course the cost of it was to make a simpler moulding than the desired one, but for practical instances.

#### Formulation, mixing procedure

In this part is described the process and parameters used for the manufacturing of the PDMS gasket. There are only one size of moulding, but the different attempts only differ in the height of every single sample. The formulation needed for the pre-polymer is followed by the Table3.8 parameters. Both elements are stirred for at least 10min until a homogeneous gel is seen (keeping in mind that both are transparent).

| base | curing agent |
|------|--------------|
| 10x  | 1x %         |

Table 3.8: PDMS Formulation: base and curing agent ratio

Later on, the mix is inserted on a vacuum chamber for degassing and get rid of the bubbles, for 30min.

#### Preparation – glass moulds

In this part the glass moulds are specified as a part of the curing step. After the mixing procedure the uncured PDMS is poured very carefully (to avoid any air droplet) into a glass mould which consist in a glass surface delimited with glass slides depending on the desired height. Carefully a Xerox® film is extended all over the liquid PDMS. The prepared filled mould is then introduced in a 75°C heated oven for 3 h. Once the PDMS is cured, it can be shaped with a razor blade to the adequate shape. Different samples can be seen in Fig.3.16

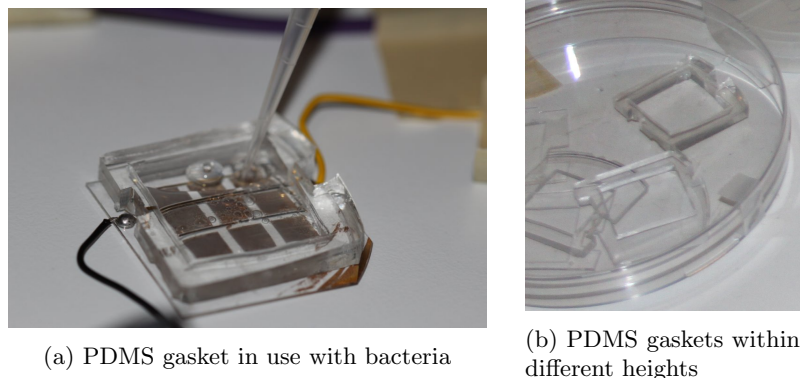


Figure 3.16: Different made PDMS gaskets

## 3.2 Gasket fabrication

---

### 3.2.3 gasket tests

In this part, it is discussed how gaskets were resulted and the problems or successful outcomes from the manufacturing process. Table 3.9 and 3.10 resembles the different times used and the polymer finish characteristics.

| One hole gasket test of 2mm |   |   |  |   |
|-----------------------------|---|---|--|---|
| Thiol monomer               | Off stoichiometry                                     | Time (s)                                    | Results                                    |   |
| PETMA                       | 50 %  | 26  | too much curing time                       | X |
|                             |   | 20  | still over-cured, no hole                  | X |
|                             |   | 15  | half well                                  | X |
|                             |   | 10  | defined well                               | ✓ |
|                             |   | 8   | more sticky, neat                          | ✓ |
|                             | 6   | very clear, uncured, affected by cover film | X  |   |
|                             | 80 %  | 27  | too much curing time                       | X |
|                             |   | 26  | still overcooked                           | X |
|                             |   | 15  | almost defined hole                        | X |
|                             |   | 10  | hole, and more clear                       | ✓ |
| 8                           |   | uncured, bottom too raw & soft, clearest    | X  |   |
| PETMP                       | 50 %  | 27  | too much curing time                       | X |
|                             |   | 20  | over-cured, no hole                        | X |
|                             |   | 15  | over-cured                                 | X |
|                             |   | 10  | still no hole, bottom uncured              | X |
|                             |   | 8   | same as 10 & no adherence                  | X |
|                             |   | 5   | half well, blurred                         | X |
|                             |   | 3   | almost defined hole, blurred, detachable   | ✓ |
|                             |   | 2   | almost defined hole, clearer, softer       | ✓ |
|                             | 1.5   | uncured, very stiff, detachable             | X  |   |
|                             | 80 %<br>(very well defined wells)<br>softer than 50 % | 27  | too much curing time                       | X |
|                             |   | 5   | almost defined hole, bottom raw, not clear | X |
|                             |   | 3   | defined hole but stretched, clearer        | X |
|                             |   | 2   | defined hole & softer, breaks easily       | ✓ |
|                             |   | 1.5   | defined hole, easier to detach             | ✓ |

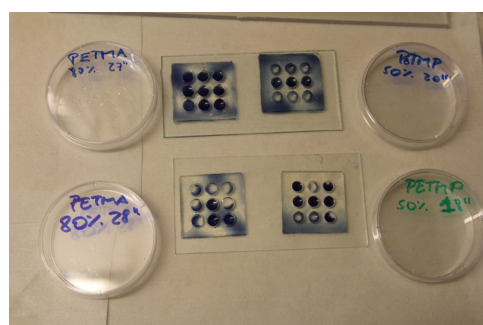
Table 3.9: Curing time variations for best OSTE 2mm sample

This parameter can be reflected on the gasket pictures in Fig.3.17

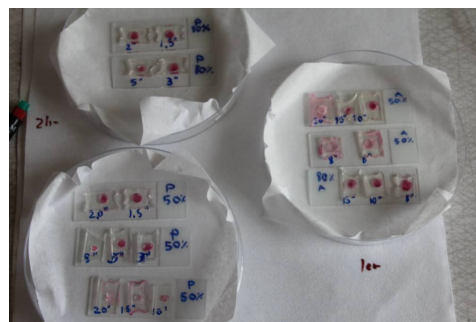
### 3 Design and assembly of the experimental setup

| One hole gasket test of 1mm |                   |          |                               |   |
|-----------------------------|-------------------|----------|-------------------------------|---|
| Thiol monomer               | Off stoichiometry | Time (s) | Results                       |   |
| PETMA                       | 50 %              | 15       | too much curing time          | X |
|                             |                   | 10       | over-cured                    | X |
|                             |                   | 6        | defined hole                  | ✓ |
|                             |                   | 4        | defined hole                  | ✓ |
|                             | 80 %              | 8        | almost defined hole           | X |
|                             |                   | 6        | a bit uncured                 | X |
| PETMP                       | 50 %              | 6        | too much curing time, no hole | X |
|                             |                   | 4        | over-cured, no hole           | X |
|                             |                   | 2        | defined hole                  | ✓ |
|                             |                   | 1        | defined hole, bit uncured     | ✓ |
|                             | 80 %              | 4        | almost defined hole           | X |
|                             |                   | 2        | almost defined hole           | X |
|                             |                   | 1        | top face stuck to cover film  | X |
|                             |                   | 0.5      | too uncured, melted           | ✓ |

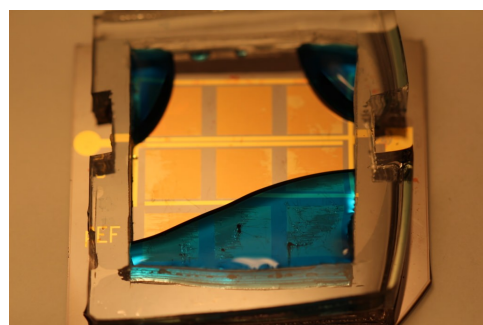
Table 3.10: Curing time variations for best OSTE 1mm sample, curing agent for PETMP 80% was 0.1g for the others 0.05g



(a) OSTE gaskets with different sealing tests



(b) OSTE one hole gaskets within different curing times



(c) 2cm PDMS gasket with sealing property on Teflon layer



(d) 1mm PDMS gasket with hydrophobic property without leaking

Figure 3.17: OSTE and PDMS gaskets on sealing tests

### 3.3 Bacteria to be used

---

**Comments** In this stage, two versions were tested. In the first one, the first problem came to discover that for very thick layers, the base remained uncured, while the top face was satisfactory. Even though, sealing tests were made on nine-holed gaskets which the best sealing was with PETMP 80% but not last for more than 1 h.

Considering that, a simple way was made by reducing the test to a single hole seen in Subsection 3.2.1. In this tests was considered mainly: hole circular shape, polymer transparency and sealing, where the best ones were:

**2mm sealing test:** PETMA 50% 10s, and PETMP 80% 1.5s.

**1mm sealing test:** PETMP 50% 1s (PETMA had not good hole shapes).

There were not enough time to return to the nine-hole test because bacterial tests came out and a gasket was required for it. Even though nine-hole tests shown not having the right curing time because on sealing tests liquid leaked from under the gasket. Fig. 3.17a

In the second version, sealing was quite good, and even with different gasket heights (5mm, 1mm) it was capable to retain the bacteria medium on top of the manufactured wafer, taking in consideration that the wafer's surface was a thin layer of Teflon. This because of its rubber-texture of the PDMS material that stick easily to the surface, but with a little help of pressure to keep bubble air out of the bottom surface of the gasket.

### 3.3 Bacteria to be used

In this part a brief description of the bacteria used and its morphology and topology.

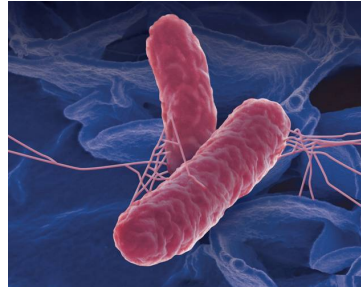
Bacteria regarding its status cause infections by sporadic or epidemic mediums[4], these can be divided in several typologies where common ones are Gram-negative bacteria and gram-positive bacteria. Considering the more resistant against antibodies between both are the gram-negative because of its several cellular layer.

#### 3.3.1 Salmonella Typhimurium

In this part salmonella is described as a specific subspecies (Serovars) of *Salmonella enterica*.

*Salmonella* species are reported as an often bacteria acquired in the community, as in Table 5 of the Infection Control Guide in Hospital Personnel[24].

The main bacterium used was *Salmonella Typhimurium* because of their well known adhesion mechanism. Another bacterium used on Teflon-glass slides, *Pseudomonas aeruginosa* also used to compare with *Salmonella*, its adhesion force on the same surface.



(a) Salmonella close up



(b) Salmonella entanglements



(c) Biofilm formation

Figure 3.18: *Salmonella typhimurium*

**Comments** Some of the problems related to the bacteria was the long period of time required to see the attachment(at least 60 min), but was not too much considering that in common DEP/EWOD experiments lasted from 3 to 7 days [25].

## Chapter 4

# Measurements and results

This section consists of three parts. The first is a numerical simulation of the DEP force experienced on particles under the influence of spaced electrodes. Different models for the particle are compared and optimal frequencies are determined for implementation. Pro and cons are discussed for DEP techniques. The second part is an experimental study of EWOD to influence the bacteria adhesion of Salmonella Typhimurium. This study is carried out in cooperation with Karolinska Institute and the group of Prof. Ute Römling. The third part is an experimental setup and several experiments for evaluating the bacteria attachment, which were performed and are discussed.

The implemented device has 5, 10 and 20  $\mu\text{m}$  electrodes have gap distances of 2.5, 5 and 15  $\mu\text{m}$  respectively.

### 4.1 Numerical simulations of DEP on bacteria model

In this part parameters for the CM plots are calculated for the bacteria planned to be used and simulations on how the gradient of electric field from two gold electrodes in a liquid solution (water) affects the model particles.

DEP simulations were studied using COMSOL simulation and complemented by MATLAB calculations for effective CM values on DEP applications. Two energized co-planar gold electrodes under a layer of Teflon with a water medium were simulated. MATLAB curves illustrating the difference of the CM factor by changing the medium where the particles are tested Fig.4.2 (different medium conductivities) as it is going to be explained in the following Subsection.

#### 4.1.1 MATLAB calculations

Here it is calculated the complex permittivity of bacteria and medium considering the biological approximation model. At the end a CM factor plot is derived. From Section 2.3.1, it is obtained data shown in Table 4.1 .

By the smeared-out sphere approximation considered in Fig. 2.6b the following formulas are derived for the bacteria analysis in MATLAB code:

| Three layer particle information |                         |                          |                                      |                     |
|----------------------------------|-------------------------|--------------------------|--------------------------------------|---------------------|
| Particle                         | Layers (outer to inner) | Radius [ $\mu\text{m}$ ] | $\sigma$ [ $\mu\text{S}/\text{cm}$ ] | $\varepsilon$ [F/m] |
| Yeast                            | 1 (cell wall)           | 2.5                      | 140                                  | 60                  |
|                                  | 2 (cytoplasm)           | 2.36                     | 0.0025                               | 6                   |
|                                  | 3 (nucleus)             | 2.35                     | 2000                                 | 50                  |
| E. Coli                          | 1 (cell wall)           | 1                        | 500                                  | 60                  |
|                                  | 2 (cytoplasm)           | 0.98                     | 0.0005                               | 10                  |
|                                  | 3 (nucleus)             | 0.975                    | 1000                                 | 60                  |

Table 4.1: Different parameter to consider on three-layer particle(E. coli density: $\rho = 1100 \text{ kg}/\text{m}^3 \pm 3\%$ )

$$\varepsilon_{BACT}^* = \varepsilon_3^* \left[ \frac{\left(\frac{r_3}{r_2}\right)^3 + 2 \left(\frac{\varepsilon_{21}^* - \varepsilon_3^*}{\varepsilon_{21}^* + 2\varepsilon_3^*}\right)}{\left(\frac{r_3}{r_2}\right)^3 - \left(\frac{\varepsilon_{21}^* - \varepsilon_3^*}{\varepsilon_{21}^* + 2\varepsilon_3^*}\right)} \right] \quad (4.1)$$

$$\varepsilon^* = \varepsilon + j \frac{\sigma}{\omega} \quad (4.2)$$

where  $\varepsilon_x$  is the permittivity of the layer  $x$ , thus  $x$  can be one layer(the third one) or a combination of layers(the first two ones); then  $\sigma$  stands for conductivity of the medium and  $\omega$  is the frequency domain of the applied  $\vec{E}$ . Last but not least  $\Re\{f\}$  is the real part of Clausius-Mossotti(CM) factor  $\{f\}$ .

It can be compared the results plotted on excel calculated values in Fig4.1b and the plot from Matlab in Fig.4.1c.

From the MATLAB calculations, using 5 different medium conductivities (2,10, 17.78, 31.62, 38, 50.62, 100 and 380  $\mu\text{S}/\text{cm}$ ) where DI water has  $2\mu\text{S}/\text{cm}$ , it is shown how the CM-frequency curves were affected by it and how Yeast and E. Coli bacteria change its pDEP and nDEP areas(explained in subsection 2.2.2) as a consequence of it.

From Fig.4.2 can be seen how yeast and E.Coli bacteria particles can change the CM values, so the range where nDEP can be used change for more range or less range in the frequency axis.

In addition to the selected medium, more common mediums to the healthcare were investigated.

**Blood conductivity** The conductivity of the blood varies depending on different blood composites: Hematocrit that reflects the red blood cells/blood volume ratio(the higher of it, the lower the conductivity); plasma is the major component which contains suspended ions(the higher of it, the higher the conductivity); electrolytes change the blood resistivity (the higher of them, the higher the conductivity); erythrocyte helps the oxygenation of the blood by diffusion, their orientation define the conductivity (at higher flow rates, the higher of it)[26].

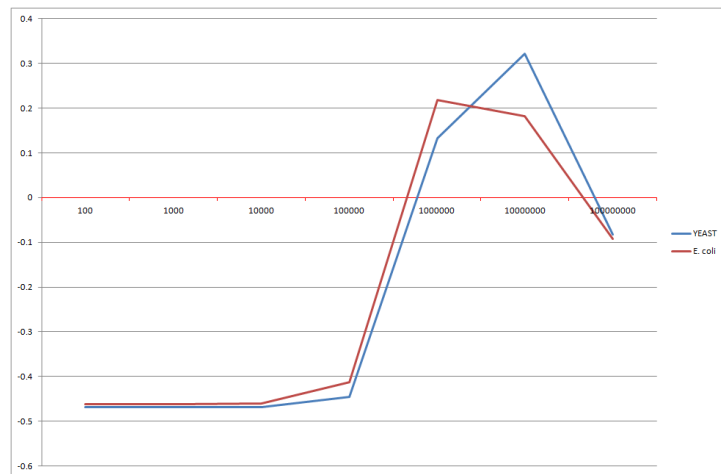
The average value by [27] experiments is 0.667 S/m.

**Urine conductivity** The conductivity of the Urine is normally around 0.028 S/m [28]

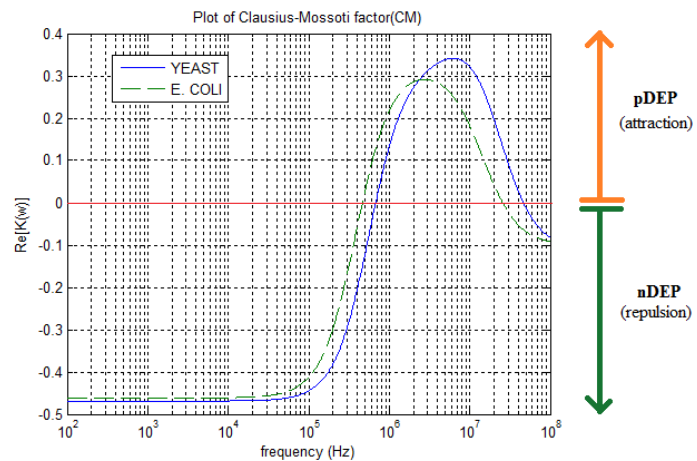
#### 4.1 Numerical simulations of DEP on bacteria model

| Frequency          | Particles | Re[CM]  |
|--------------------|-----------|---------|
| 10 <sup>2</sup> Hz | YEAST     | -0.4687 |
|                    | E. coli   | -0.4614 |
| 10 <sup>3</sup> Hz | YEAST     | -0.4687 |
|                    | E. coli   | -0.4614 |
| 10 <sup>4</sup> Hz | YEAST     | -0.4685 |
|                    | E. coli   | -0.4609 |
| 10 <sup>5</sup> Hz | YEAST     | -0.4448 |
|                    | E. coli   | -0.4127 |
| 10 <sup>6</sup> Hz | YEAST     | 0.1325  |
|                    | E. coli   | 0.2174  |
| 10 <sup>7</sup> Hz | YEAST     | 0.3216  |
|                    | E. coli   | 0.1821  |
| 10 <sup>8</sup> Hz | YEAST     | -0.082  |
|                    | E. coli   | -0.0917 |

(a)  $\Re\{CM\}$  from frequency



(b) Excel plot for general idea



(c) Matlab plot for detailed data

Figure 4.1: CM plots from Excel and Matlab calculations

**Saliva conductivity** Its permittivity for low frequency is almost constant ( $<3\text{GHz}$ ): the real part is 6.8 and the imaginary 1 in average[29]. To translate to conductivity is: 0.628 S/m very similar to the blood.



## 4 Measurements and results

---

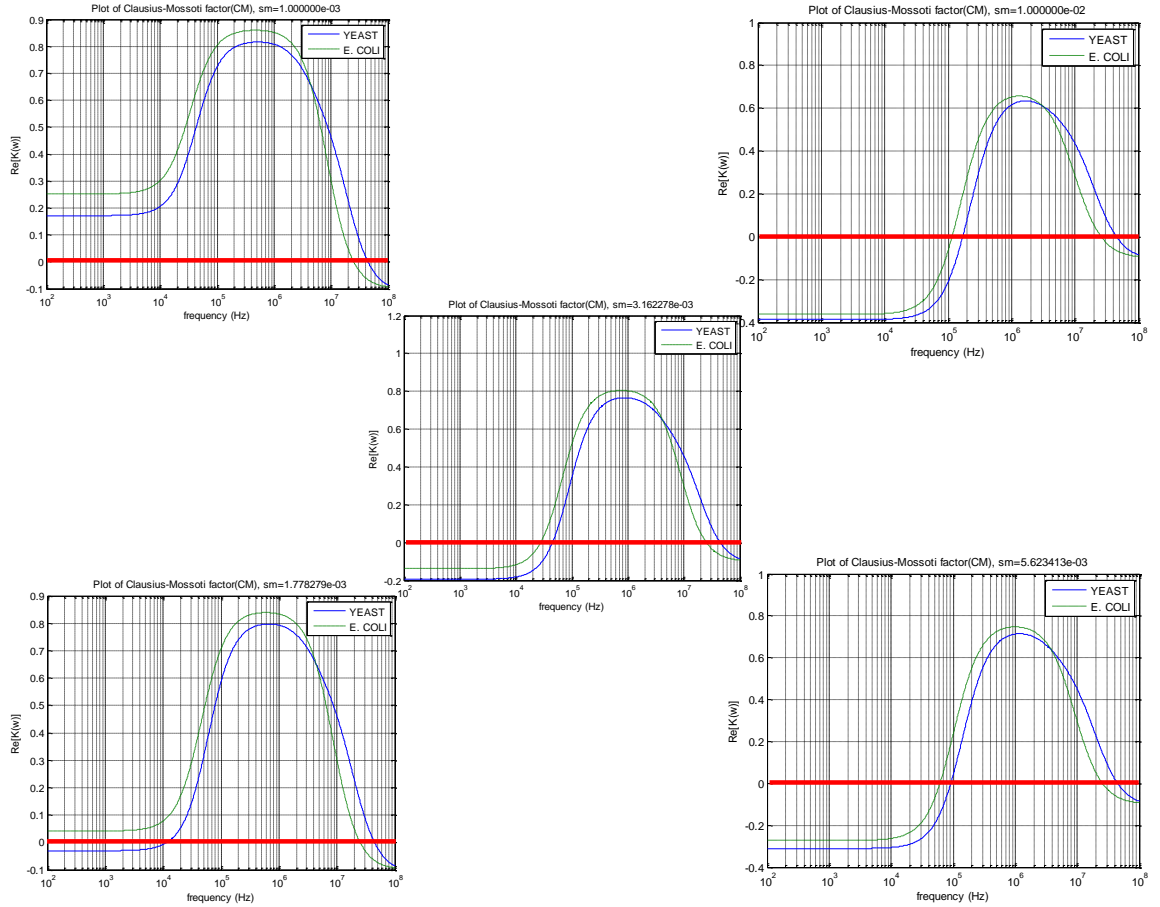


Figure 4.2: CM of particles on different conductivity mediums

### 4.1.2 COMSOL analysis and results

In this section, a complete simulation about how electric field acts on two coplanar wave-guide geometry electrodes is described. Here DEP force is the main active force and the direct relation with the frequency is portrayed.

From the COMSOL simulations, there were two measurements of electric potential intensity, electric field intensity and DEP force on the medium, as presented on Fig4.3, Fig.4.4 and Fig.4.5 respectively.

In all pictures of Fig.4.5: the main reject force was the one at 1kHz and from the attraction forces, three were the main ones which:  $F(3.33\text{MHz}) < F(6.67\text{kHz}) < F(10\text{MHz})$ .

## 4.1 Numerical simulations of DEP on bacteria model

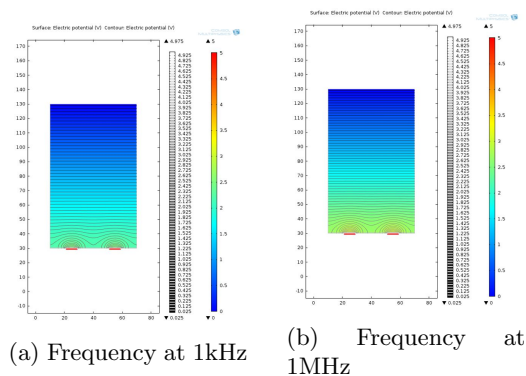


Figure 4.3: Electric Potential intensity in 8  $\mu\text{m}$  electrodes width

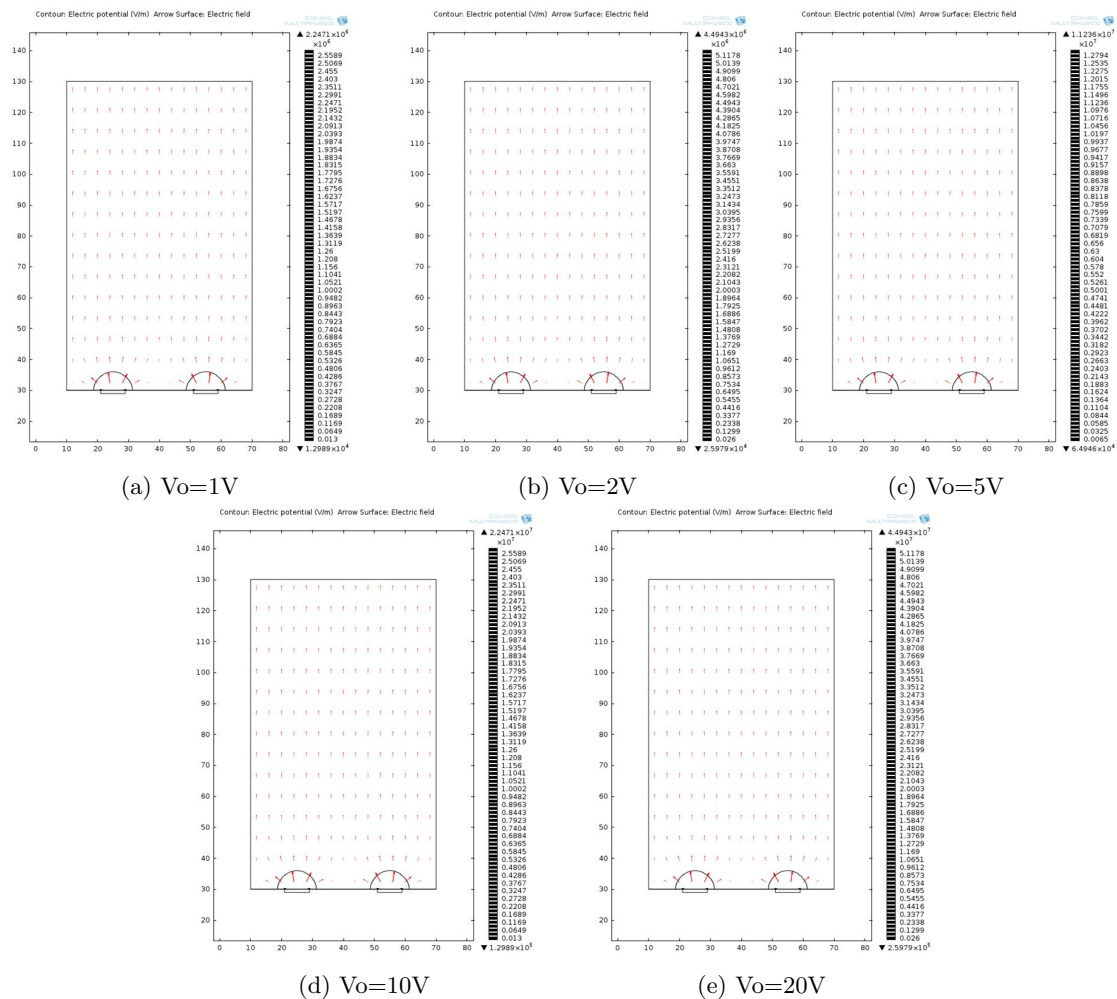


Figure 4.4: Electric Field intensity at different potentials

## 4 Measurements and results

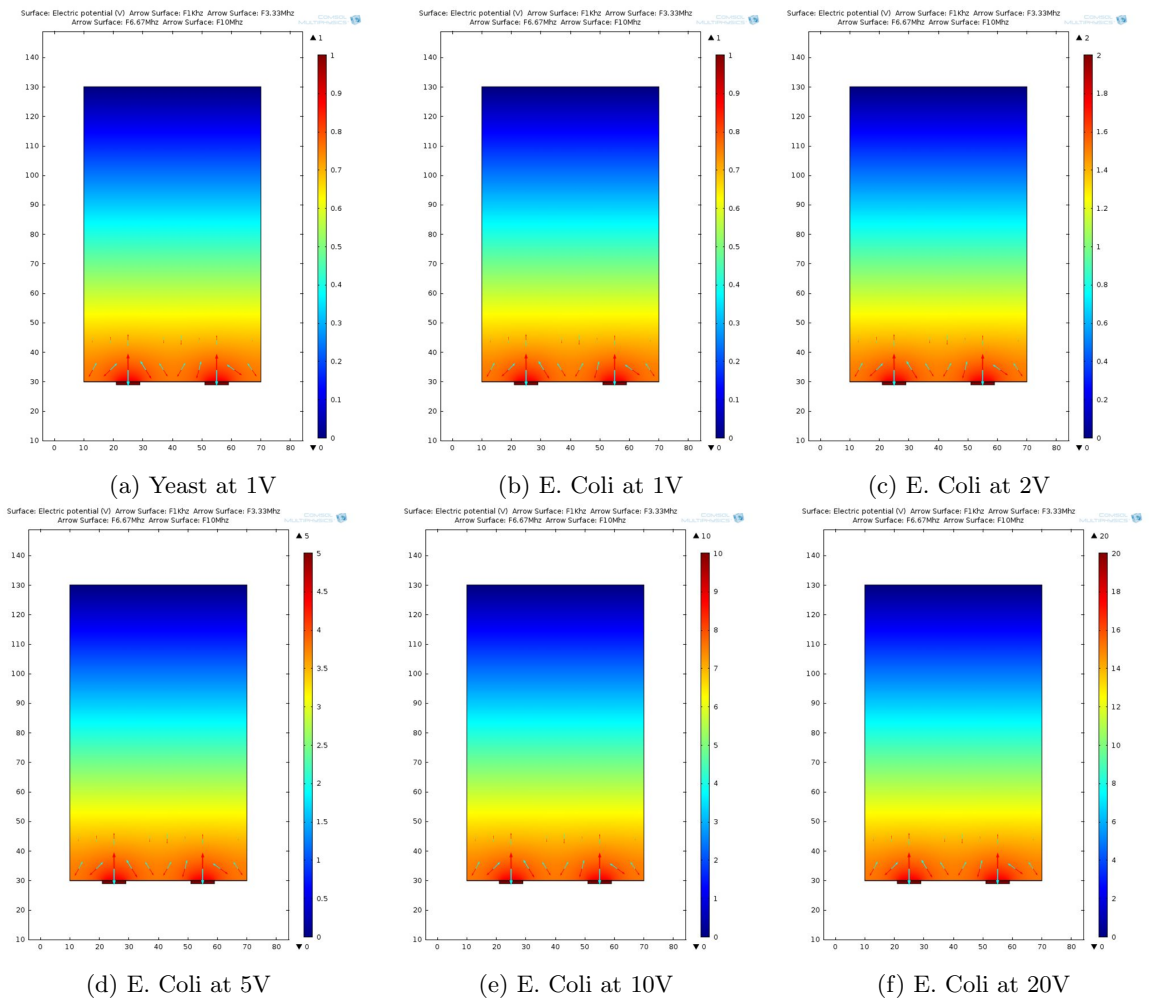


Figure 4.5: DEP Force at different particles and potentials

**Bacteria rejection possibility** Based on the presented electrical field simulations, it can be calculated if bacteria rejection is viable.

The particle used in the COMSOL simulation was Yeast at a frequency of 100Hz. The real part of Clausius-Mossotti factor used for this particle was -0.4687 considering the negative sign as the zone of the attraction for DEP as it can be seen in Fig.4.1c.

The CM factor was calculated using MATLAB, where medium was DI water (conductivity from COMSOL 38mS/m) and the yeast was considered as a 3-layer permittivity particle, which resulted in complex permittivities  $1.1746 \times 10^{-8} - i2.5778 \times 10^{-6}$  and  $7.0834 \times 10^{-10} - i6.0479 \times 10^{-5}$  (F/m) for yeast and water respectively.

The start point is the Einstein– Smoluchowski relation from the Kinetic theory [30] which describes the Brownian motion on a medium.

The general equation is the Eq.4.3.

$$D = \mu \kappa_B T \quad (4.3)$$

where  $D$  is the diffusion constant,  $\mu$  is the mobility,  $\kappa_B$  is the Boltzmann's constant and  $T$  is the absolute temperature.

It can be found diffusion bacteria values like: Pseudomonas aeruginosa ( $2.1 \times 10^{-9}$  m<sup>2</sup>/s), Klebsiella pneumoniae ( $0.9 \times 10^{-9}$  m<sup>2</sup>/s)[31] and Escherichia coli ( $0.8 \times 10^{-12}$  m<sup>2</sup>/s)[32]. Considering room temperature ( $T = 300$ K) and the Boltzmann's constant ( $\kappa_B = 1.3807 \times 10^{-23}$  m<sup>2</sup>.kg/s<sup>2</sup>.K) and replacing the diffusion values on Eq.4.3 mobilities are obtained: Pseudomonas aeruginosa ( $5.1 \times 10^{11}$  m/Ns), Klebsiella pneumoniae ( $2.2 \times 10^{11}$  m/Ns) and Escherichia coli ( $1.9 \times 10^8$  m/Ns).

From the general equation is derived also mobility as particle's *drift velocity*( $v_d$ ) to an applied force ( $F$ ) Eq.4.4 [33]

$$\mu = \frac{v_d}{F} \quad (4.4)$$

where the acting force is evaluated through the gradient of the squared electric field on the vertical axis ( $\nabla |\vec{E}_y|^2$ ), due to see the effective force that is going to act on the bacteria.

Velocity is going to be calculated by the multiplication of both variables in Eq.4.4

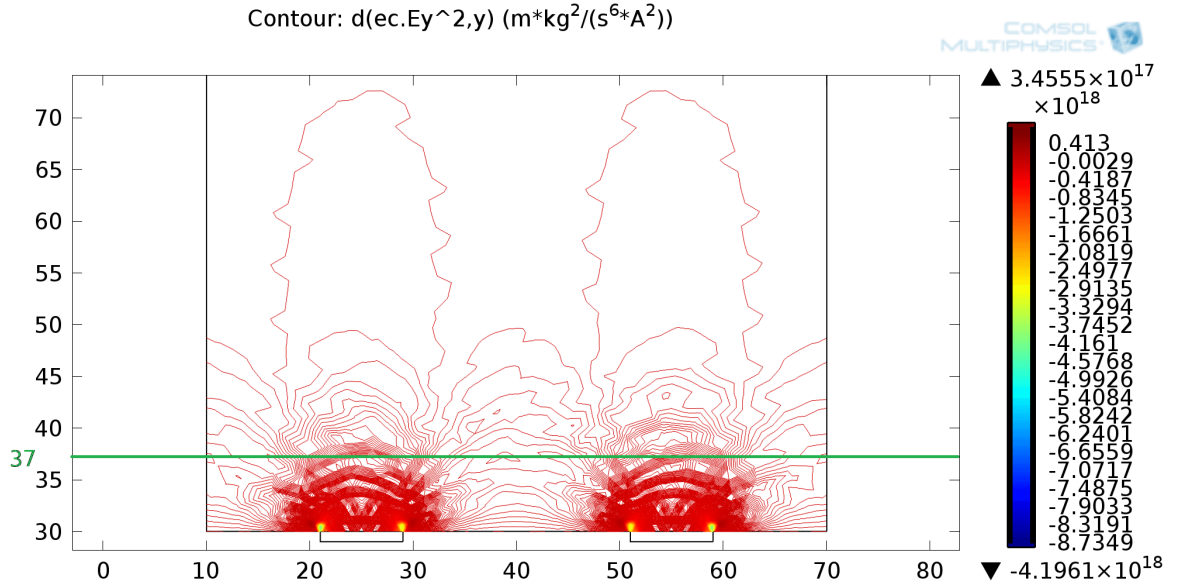
From COMSOL pictures in Fig.4.6, it can be seen that in Fig.4.6a  $\nabla |\vec{E}_y|^2$  keeps the same shape while its values increase as the potential voltage is increased. The highest values of  $\nabla |\vec{E}_y|^2$  are on top of the electrodes going into the diagonal direction while the lowest are very near the electrodes edges. This electric field intensity analysis can complement also the distance effect seen in Fig.2.5

From the resulted mesh it can be considered  $7\mu\text{m}$  of distance (height) from the electrodes as an acting DEP force effect.

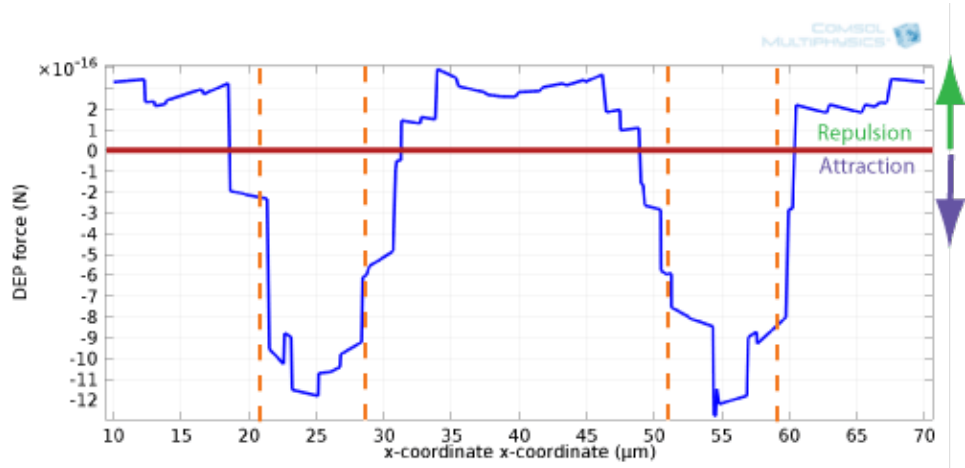
Next, in Fig.4.6b shows the DEP forces at  $7\mu\text{m}$  of distance along the x axis.

Using Eq.2.4 and COMSOL  $\nabla |\vec{E}|^2$  values, DEP force is calculated in Table.4.2 considering radius of the particle (bacteria)  $r = 0.5\mu\text{m}$ , vacuum permittivity  $\epsilon_o = 8.854 \times 10^{-12}$ , water medium  $\epsilon_m = 80.1$ ,  $\Re\{CM\} = -0.4687$  extracted from MATLAB calculations.

Replacing values from Table.4.2 into Eq.4.4, and using the mobilities of each bacteria, the Drift velocity of the particle (bacteria) is illustrated in Table.4.3



(a) Distance to consider as space of rejection,  $7\mu m$



(b) DEP forces at  $7\mu m$  above the electrodes

Figure 4.6: COMSOL DEP simulation - Electric field analysis

Comparing the velocity obtained to the Diffusion length, which defines how far the concentration is dispersed in a medium during a period of time. It is defined by Eq.4.5[34].

$$L = 2\sqrt{D t} \quad (4.5)$$

Replacing the Diffusion values of the bacteria can be seen on Table.4.4 the common length that moves during one second.

In comparison to the values obtained in Table.4.3, the numerical simulations provides more speed due to the DEP force compared with the calculated by control negative movement(without any applied force).

#### 4.1 Numerical simulations of DEP on bacteria model

---

| Potential<br>(V) | DEP force                 |                          |
|------------------|---------------------------|--------------------------|
|                  | @max. height(N)           | max.found value(N)       |
| 1                | $-3.5788 \times 10^{-19}$ | $3.2093 \times 10^{-16}$ |
| 2                | $-1.4315 \times 10^{-18}$ | $1.2837 \times 10^{-15}$ |
| 5                | $-8.9470 \times 10^{-18}$ | $8.0233 \times 10^{-15}$ |
| 10               | $-3.5788 \times 10^{-17}$ | $3.2093 \times 10^{-14}$ |
| 20               | $-1.4315 \times 10^{-16}$ | $1.2837 \times 10^{-13}$ |
| 30               | $-3.2209 \times 10^{-16}$ | $2.8884 \times 10^{-13}$ |

Table 4.2: DEP force calculated from COMSOL simulations

| Potential<br>(V) | Pseudomonas aeruginosa |                      | Klebsiella pneumoniae |                      | Escherichia coli       |                      |
|------------------|------------------------|----------------------|-----------------------|----------------------|------------------------|----------------------|
|                  | min.(m/s)              | max.(m/s)            | min.(m/s)             | max.(m/s)            | min.(m/s)              | max.(m/s)            |
| 1                | $-1.8 \times 10^{-7}$  | $1.6 \times 10^{-4}$ | $-7.8 \times 10^{-8}$ | $7.0 \times 10^{-5}$ | $-6.9 \times 10^{-11}$ | $6.2 \times 10^{-8}$ |
| 2                | $-7.3 \times 10^{-7}$  | $6.5 \times 10^{-4}$ | $-3.1 \times 10^{-7}$ | $2.8 \times 10^{-4}$ | $-2.8 \times 10^{-10}$ | $2.5 \times 10^{-7}$ |
| 5                | $-4.5 \times 10^{-6}$  | $4.1 \times 10^{-3}$ | $-1.9 \times 10^{-6}$ | $1.7 \times 10^{-3}$ | $-1.7 \times 10^{-9}$  | $1.5 \times 10^{-6}$ |
| 10               | $-1.8 \times 10^{-5}$  | $1.6 \times 10^{-2}$ | $-7.8 \times 10^{-6}$ | $7.0 \times 10^{-3}$ | $-6.9 \times 10^{-9}$  | $6.2 \times 10^{-6}$ |
| 20               | $-7.3 \times 10^{-5}$  | $6.5 \times 10^{-2}$ | $-3.1 \times 10^{-5}$ | $2.8 \times 10^{-2}$ | $-2.8 \times 10^{-8}$  | $2.5 \times 10^{-5}$ |
| 30               | $-1.6 \times 10^{-4}$  | $1.5 \times 10^{-1}$ | $-7.0 \times 10^{-5}$ | $6.3 \times 10^{-2}$ | $-6.2 \times 10^{-8}$  | $5.6 \times 10^{-5}$ |

Table 4.3: Drift velocity for different bacteria

| Diffusion Length (m)  | Bacteria               |
|-----------------------|------------------------|
| $9.17 \times 10^{-5}$ | Pseudomonas aeruginosa |
| $6.00 \times 10^{-5}$ | Klebsiella pneumoniae  |
| $1.79 \times 10^{-6}$ | Escherichia coli       |

Table 4.4: Diffusion length of bacteria during one second

## 4.2 Experiments of EWOD surfaces on live bacteria

In this section EW tests are described. First CA measurements in a single plate with a single tip are used to calculate which voltage is the ideal for a more strong EW effect. Furthermore, different waveforms voltages were used to see the difference in that as well.

### 4.2.1 Contact angle tests

In this section several measurements are displayed: CA vs. time to observe evaporation effect and CA vs. Voltage within different mediums to see the effect of volts and its difference with theoretical curve.

In order to learn and predict the EWOD behaviour of the particles in general mediums, potential applications were done to find the best voltage to use. Contact angle measurements were made on a simple setup: from the bottom a conductive medium (a sheet of double side 12 $\mu$ m copper in a 8mm printed circuit board, PCB) then a dielectric layer (two-side *Si* and *SiO<sub>2</sub>* wafer covered with Teflon) and a very narrow surface with applied potential (metal tip to conduct the applied voltage) as shown in Fig.4.7.

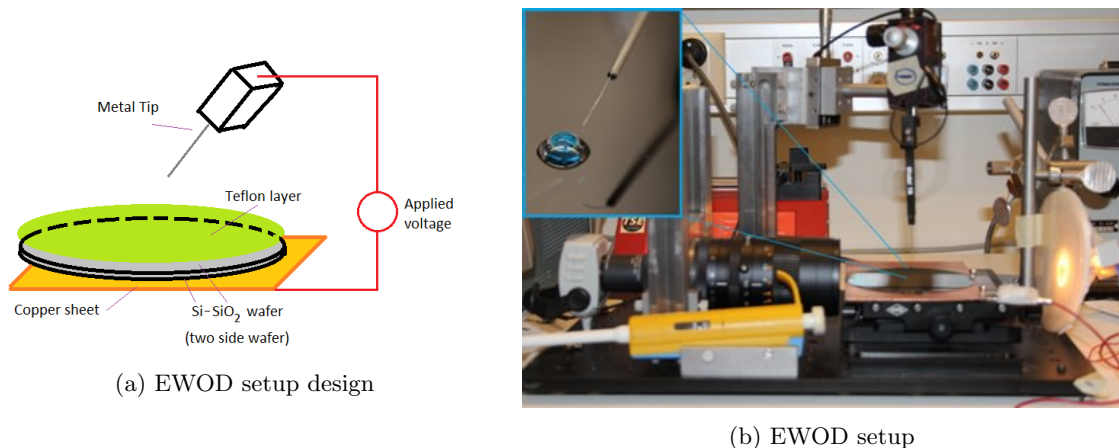


Figure 4.7: EWOD setup for CA measurements

*Setup used:* Camera of 1.3 M Pixel USB2.0 Moticam 1000; CANON TV zoom lens V6x16 16-100mm 1: 1.9; C-MOUNT COSMICAR TV lens extension tube set which connect zoom lens with Camera 40mm; SELTRON PS 1715 DC power supply, 0-25V 2A for a 3V bulb light; a FINNPIPETTE pipette from 0-40 $\mu$ L; and a SIGNATONE 393-J Tomkins Ct. probe, Model S-725-CRM, tip model 7A.

## 4.2 Experiments of EWOD surfaces on live bacteria

---

**Droplet evaporation tests** Having calculated the droplet evaporation over time can show how contact angle changes and the volume too. This helped to see how evaporation impacts on contact angle measurements during time without considering the effect of EWOD, as shown in evaporation curve of Fig.4.8. Electrowetting droplet on time also have been studied but on parylene HT films rather than Teflon layer, where stability is proved by more dielectric failure resistance compare to parylene C and durability (up to 6h) in oil medium[35].

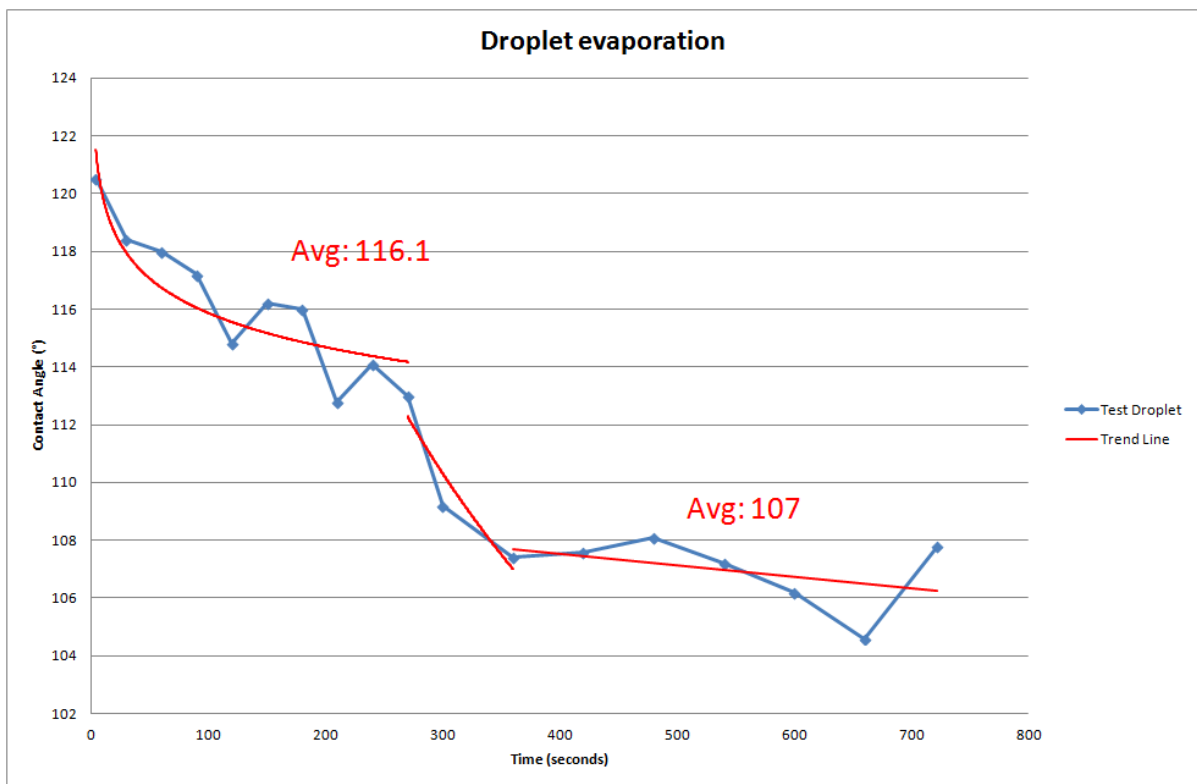


Figure 4.8: Contact angle measurement vs. time within evaporation



**Contact angle tests by applied potential** Using different mediums at different DC potentials, it was discovered how the experimental curve differed from the theoretical, and reached a limit in which electrolysis was achieved. Fig.4.9

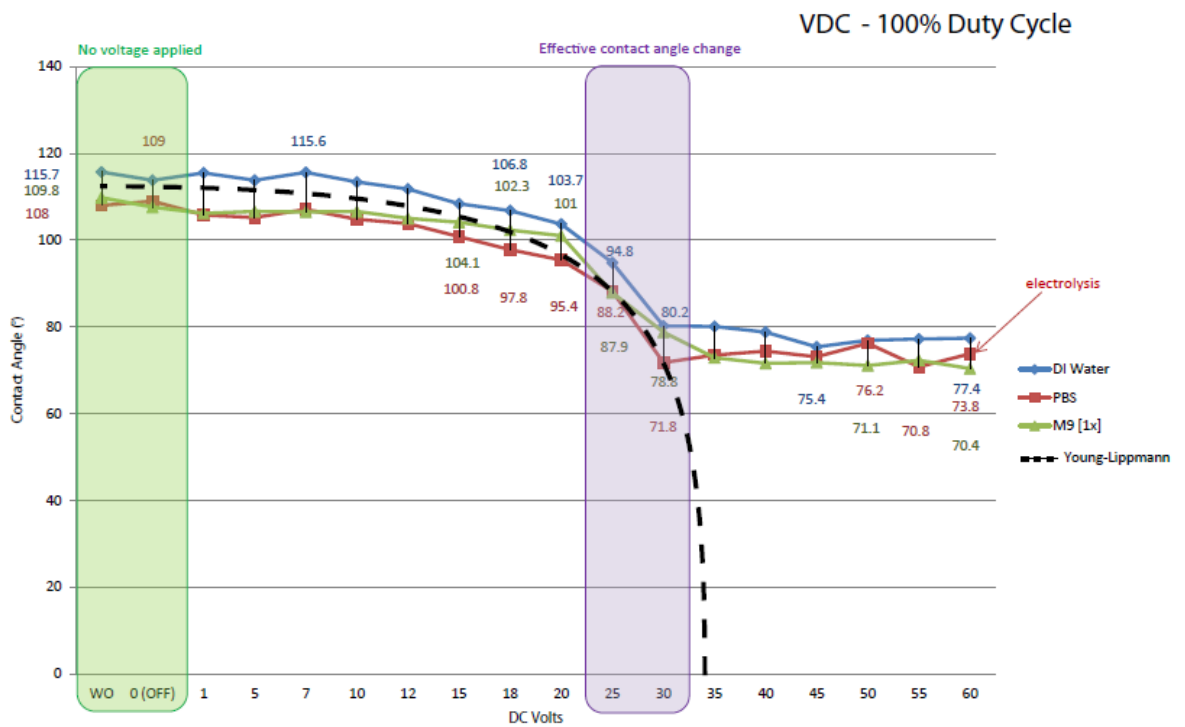


Figure 4.9: Contact angle vs. voltage within different mediums and theoretical curve

Theoretical curve by Young-Lippmann in wetting capillarity described by equation Eq.2.6 in Subsection2.2.3 is shown in Fig.4.9, where contact angle saturation is not contemplated by theory but is clearly observed in practice until dielectric layer breakthrough.

### 4.2.2 Waveform tests

In this section CA measurements vs. CA change steps within different waveforms are displayed and discussed.

Measurements done by a function generator changing between different waveforms to see the improvements on EWOD applications not only on the AC voltage change.

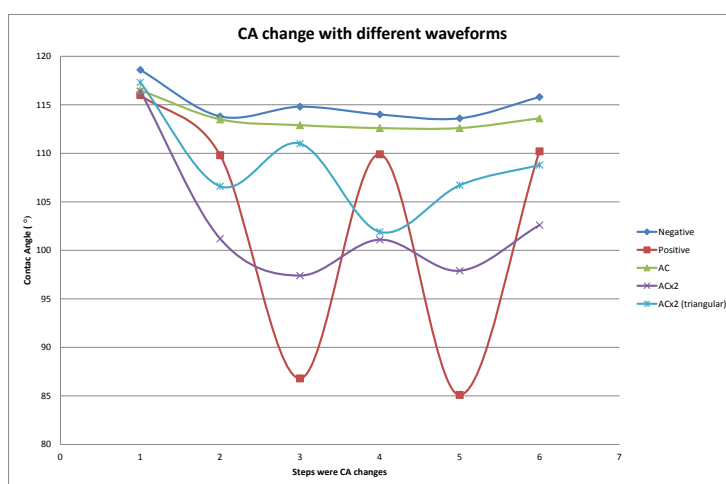


Figure 4.10: Highest effect of waveforms on CA measurements

From Fig.4.10, it is shown that the more extreme CA change is made by positive waves, which squared waves were used keeping the negative charge potential on top of the droplet.

## 4.3 Bacteria tests

In this part, in order to continue with the proof of anti-fouling process of the chips, bacteria tests were made on Karolinska institute labs, and detailed with the problems that were found, such as measurement facilities and convenient setup, and the future ideas for better results. All processes are included.

Bacteria tests on adhesion has been studied in other papers, but none of them focused on antibacterial surfaces, where electrodes wafer were hanging on a bacteria medium for several hours[25]. In this case, it is used electrowetting [22] (based on an open wire-free design) (and DEP is disregarded due calculate the medium and bacteria conductivity to sync with their CM frequency).

Bacteria tests have been carried out on Karolinska labs, using LEICA DMRE microscope and HAMAMATSU dual mode cooled CCD camera C4880. This microscope uses lens 4 lenses:  $\infty/0.17/D$ , 20x/0.5, 63x/1.32-0.6 (oil based) and 100x/1.25, where the last one is the used for observing bacteria.

A Filter #7 is used (FITC=SP-101) for bacteria fluorescence viewing. The picture management program is HiPic-32 version6.4.0(Hi Performance Image control system). This setup can be seen in Fig.4.11.

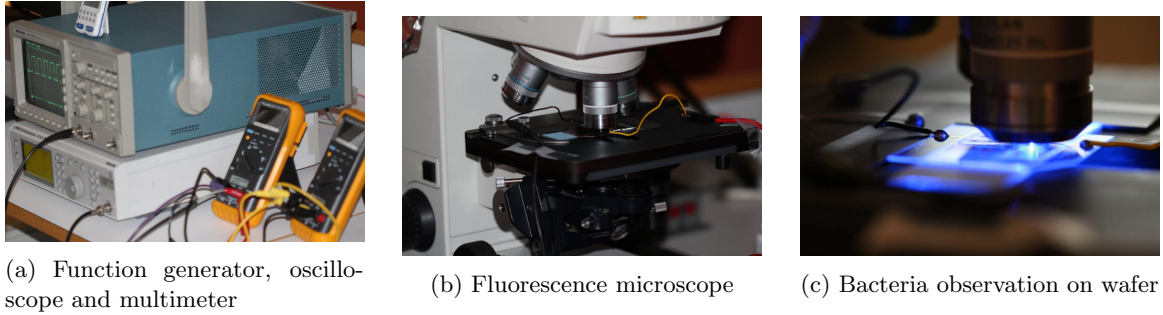


Figure 4.11: Setup used for bacteria tests

One of the problems from the beginning was to clump the glass wafer into a microscope glass slide because LEICA® microscope has a glass slide holder. But with some PBS as medium has been controlled.

In the interest of having a better way to refer the chip interdigitated electrodes blocks, it has being assigned a number, and it is shown also which wafers were used according to the size of the “finger” electrodes.Fig.4.12

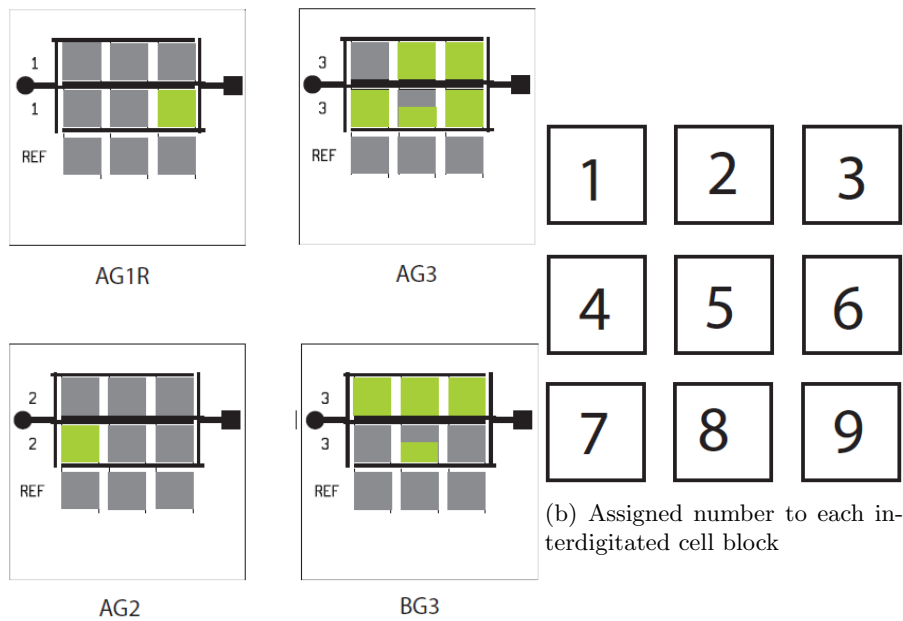


Figure 4.12: Electrodes' cells numbered and labelled

Bacteria tests were performed using Phosphate buffered saline (PBS) and M9 minimal medium - minimal microbial growth medium (M9)(1x) as medium, where M9(10x) is diluted

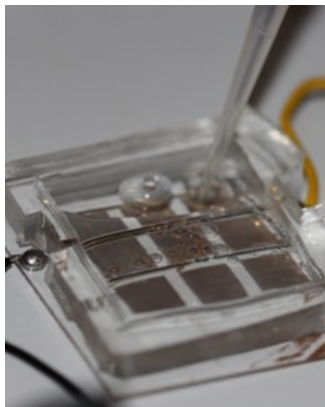
### 4.3 Bacteria tests

---

to obtain (1x). There are presented some effects of voltage on bacteria medium, but not adhesion of bacteria was observed.

Procedure:

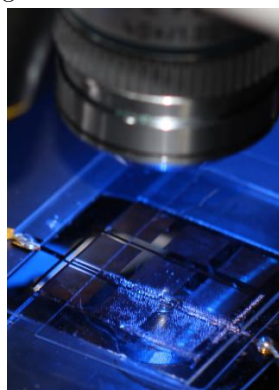
1. Turn on the chip by applying the desired voltage.
2. Stick PDMS gasket
3. pour the medium with the bacteria
4. wait for 30min
5. wash away bacteria medium and replace with clear one.
6. Pictures are taking in a clockwise order from up to bottom and left to right, taking the reference the up left corner of the electrodes block.(Having a resolution grid of 0.3, 0.6, 1 and 2 mm in the microscope cover slip stand). Fig.4.13 shows different stages at the tests procedure.



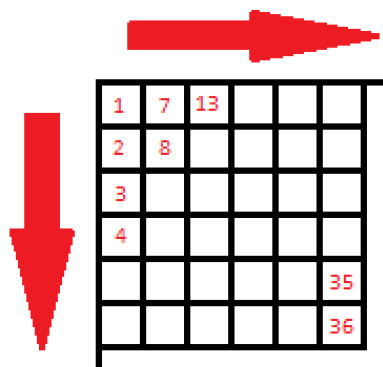
(a) Pouring medium on active chip with gasket



(b) Complete Setup: Oscilloscope, amplifier, countdown timer, multimeters and function generator



(c) Bacteria tests under luminescence light



(d) Proceeding to take pictures

Figure 4.13: Bacteria tests stages

#### 4 Measurements and results

In this way percentage of bacteria around the block can be calculated and have a real estimation of the rejection of bacteria by the active electrodes.

- Count the bacteria for each picture and making a table of the quantitative measure per electrodes block. Compare quantities of control negative blocks and active ones.

At the beginning the bacterial concentration was fixed, while the attachment of the bacteria on the surface was seen after 30 min of incubation.

To test whether the bacteria can attach to the Teflon surface (negative control), adhesion experiments on glass slides with and without Teflon covered on were performed. Two bacteria were tested, *Salmonella Typhimurium* and *Pseudomona Aeruginosa*.

For 30 min adhesion, there were no bacteria attached to the Teflon surface compared to glass slide (without Teflon covered on) which showed many cells of bacteria attached on the surface.

The adhesion time was increased to 24 h which it shown the bacteria on the Teflon surface. Therefore bacteria, both *Salmonella Typhimurium* and *Pseudomona Aeruginosa*, can attach to the Teflon surface at 24 h but not at 30 min. This may suggest that incubation time for only 30 min may not be enough for creating negative control biofilm adhesion on Teflon covered surfaces as it can be observed in Tab.4.5.

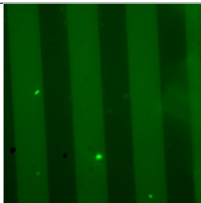
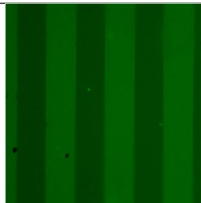
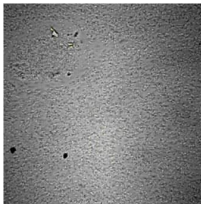
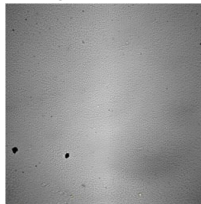
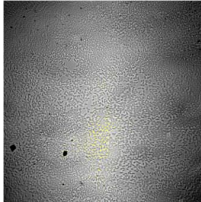
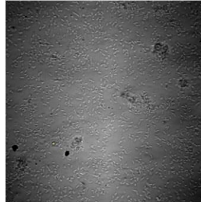
| Surface                         | Time for adhesion | After washing   |  | Results                           |
|---------------------------------|-------------------|---|--|-----------------------------------|
| Chip                            | 30 min            |  |  | Inconclusive in terms of adhesion |
|                                 |                   | Active with potential   | Negative control   |                                   |
| Glass slide covered with teflon | 30 min            |  |  | No bacteria attached              |
|                                 |                   | <i>Salmonella Typhimurium</i>   | <i>Pseudomona Aeruginosa</i>   |                                   |
|                                 | 24 h              |  |  | Attached bacteria                 |
|                                 |                   | <i>Salmonella Typhimurium</i>   | <i>Pseudomona Aeruginosa</i>   |                                   |

Table 4.5: Bacteria adhesion tests done in Karolinska laboratories

## 4.4 Discussion

In this part a final discussion of all the measurements and tests is presented to indicate a better conclusion.

**DEP Numerical simulations** From the MATLAB calculations the best curve selected was at a  $380\mu\text{S}/\text{cm}$  medium conductivity with yeast and E. Coli bacteria multi-shell value parameters using the smeared-out sphere approach Subsection.2.3.1

From the COMSOL simulations, at different used frequencies at very high frequencies (more than 100 kHz) electric field intensities reject particles and the higher the frequency more intense in the vicinity and smoother the electric potential curve over the electrodes.

Even when was not used as a antifouling method, it has been demonstrated that DEP is viable way to repel bacteria by keeping medium synchronized to great range of frequency, in order to embrace most of the bacteria types.

From picture Fig.4.6a, the gradient of the squared electric field is repulsive between both electrodes but not over them.

Furthermore, Fig.4.6b shows the DEP force along the x axis at a constant distance from the electrodes ( $7\mu\text{m}$ ); this clarify the behaviour of the forces that can reject the bacteria, as the distance become much shorter the forces increase exponentially, as well as for the voltage applied as it is seen in Table4.2.

From DEP numerical simulation it is possible to reject bacteria because shown forces along an horizontal axis can hold an almost uniform reject force value, and can be increased by the applied voltage; but it is needed to improve the configuration by having closer spaced electrodes and with smaller width, allowing forces to exerted repulsion more uniformly along the surface.

**EWOD surfaces experiment** Contact angle measurements on time within droplets evaporation was important to notice a trend line and discard future possible effect of evaporation on EWOD contact angles due only by the voltage applied and the lasted time. During the first 60s of the test, evaporation can be neglected, also in this control negative test, helped to know that the electrode tip has an effect on contact angle measurements but still can be neglected because of the very little CA change compared to the ones on the experimental curve.

The discovering of the experimental curve above the theoretical one in Fig.4.9, give as the best value of voltage to applied EWOD and with the suitable medium which was M9 medium, even though DI water has better contact angle change M9 was similar to it and works better for bacteria grow-enhancing medium. Nevertheless, droplet on EWOD has same behaviour within different mediums, but strong change in contact angle.

From the contact angle measurements I have discovered that electrolysis can be avoided for voltages higher than 16VDC by inserting the tip before it is charged, otherwise the surface tension acts as a conductive medium breaking the Teflon layer.

In the other hand, every CA angle measurement requires a new Teflon spinning because of the breakthrough of it. Dielectric failure (dielectric breakdown) as in Fig.4.14a can occur even at low voltages due to the use of ionic solutes (as well of the Double layer effect), this can be avoided with the use of larger ions size (adding specific surfactant or larger polar molecules solutions than water). It is important to highlight that the dielectric strength of the dielectric

layer become higher as the thickness increase; in the other hand, more voltage would be needed to have the same EWOD effect.

Hysteresis have been seen, so after applying voltage to reach higher voltage potential takes less time than arriving from zero potential, this due to droplet keeps charged and uncharged very slowly (capacitor behaviour). Applied voltage in electro-wetting is also time-dependent, as time goes by, higher voltage is needed to see some effect on the droplet, as in Fig4.14b.

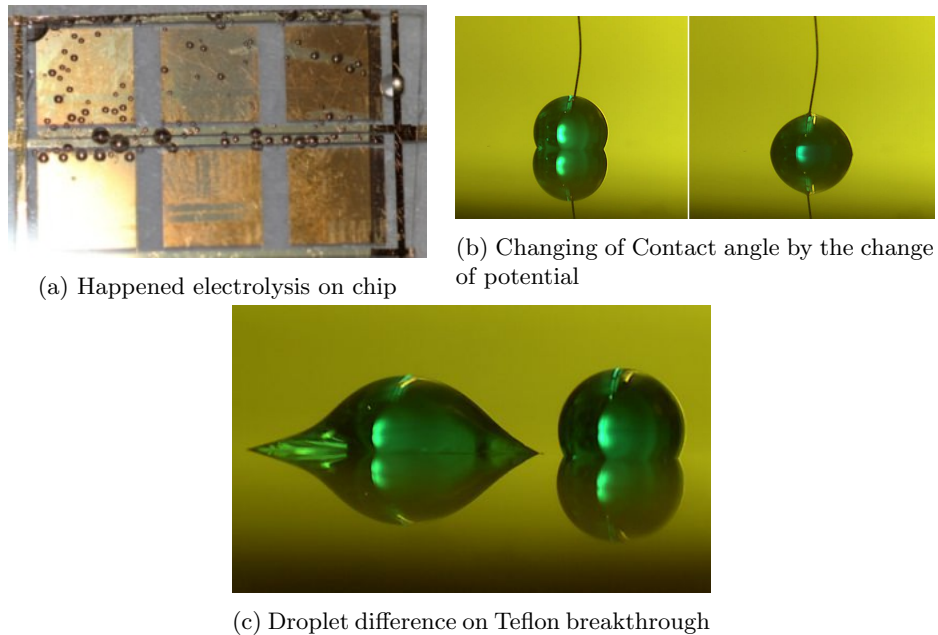


Figure 4.14: Effects of EWOD on tests

At lower range of voltages ( $< 100V$ ) using +DC, -DC, 60Hz, 1kHz or 10kHz has not much difference in the contact angle changing. But for sure the saturation point can be shortly achieve firstly in the first cases and the latter at lower frequencies. (Nanayakkara, 2010)

As for the waveform test, the waveform select was the obvious one but needed to be confirmed by these tests, the step square one but with the negative potential on top of the surface as can be seen on Fig.4.10. In addition to that, it has been demonstrated that changing Duty cycle in a square signal reduces EWOD effect on the contact angle, and considering that test, it has been observed that droplet behaviour is more effective with different duty cycles independent of their applied voltage. (Studied Duty cycles: 1%, 40%, 60% and 100%).

New designs at macro level were built, but were also used as a reference because at those distances DEP forces and E field intensity are very low, more on Appendix G.

**Bacteria tests** Bacteria tests were done in the medium, and while there were floating EP and DEP effects displayed. Some of the inconvenient was not starting with a planning observation method, as the electrodes were too little, taking pictures with the fluorescent microscope was too sensitive at movements.

About the used microscope, neither helped the fact it was oil-based lens with exert some pressure over the chip and gasket making a chamber of filled medium, this acted as a liquid

lens making more difficult the observation from top.

From the pictures in Fig.4.15 can be seen that bacteria get trapped on some electrodes due to the EP effect from the electrodes. This can helped also to sediment bacteria biofilm in areas where electrodes are not covering. Having a gasket makes LIVE observation more difficult as the diffraction in the oil lenses of the microscope increase.

It should be considered how wafer started to deteriorate as electrolysis occurs at higher levels of voltage.

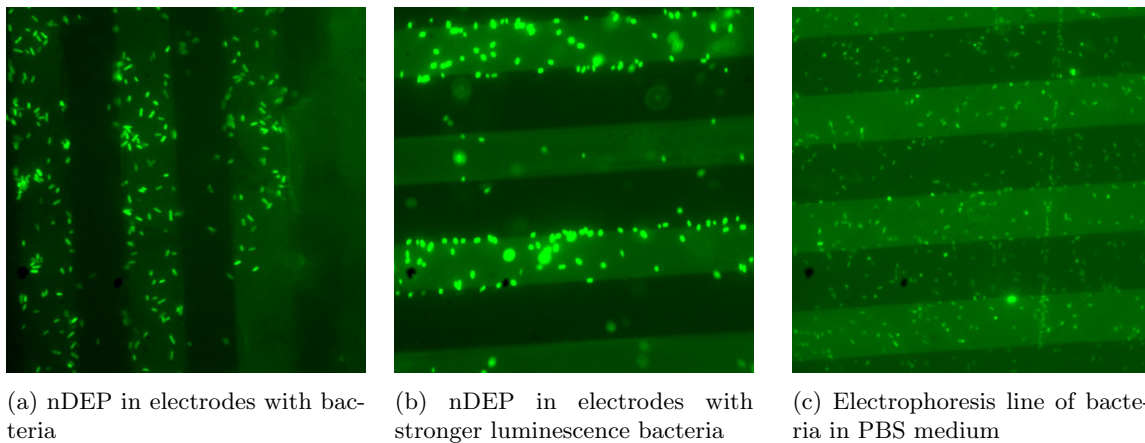


Figure 4.15: Bacteria tests on with interdigitated electrodes



## Chapter 5

# Conclusion

In this part the most important points and acquired knowledge are shown.

This project achieved the study electrokinetic micro-environments effect on determined surfaces and partially in bacteria adhesion. Even though cannot be proof that this can be an ideal antibacterial surface, a considerable step was achieved by determining its ability to do it. Further tests are remain to be done but the studies remains.

First of all, an electrodes array deposited by metal sputtered in a translucent medium was manufactured successfully with lithography-diced process in the KISTA cleanroom laboratory, one of the KTH facilities.

Referring to the second piece of the test device (with the purpose of sealing bacteria medium), gasket was manufactured in two materials: OSTE and PDMS, where the second one becomes to be the last and final version to be tested on bacteria.

In order to finished the assembly of the final testing device, a Teflon layer was uniformly spanned on the top surface with a desired height, and covered with the PDMS gasket for pouring the selected bacteria on its medium, which sealed perfectly when assembled.

Into the numerical simulations, MATLAB resulted to be a perfect complement to find the complex values needed to simulate on COMSOL. Only DEP physics where studied on this virtual environment and contact angle measurements were made to predict the EWOD behaviour.

By experiments on surfaces, contact angle measurements where crucial for knowing the EWOD behaviour for M9 medium at 30 VDC in which contact angle change dramatically and remain almost constant until droplet breakthrough (electrolysis). It was also important to consider a square waveform for input but keeping in mind to put the negative potential in direct contact of the medium (on the top electrode rather than the bottom).

Applied voltage in electro-wetting is also time-dependent, as time goes by; higher voltage is needed to see some effect on the droplet. A limitation is presented as it requires spinning Teflon for every new measurement due to the breakthrough (Teflon weakness).

From the bacteria tests can be seen that results were shown in some sections of the electrodes because the entropy of the bacteria; EP and DEP behaviour were observed from the electric field effects. One of the biggest challenges was to apply two theories and mixed them in a simple test based on the surface energy of the manufactured chip.

## 5.1 Project summary

In this part, a less detailed summary of the thesis is presented and described.

- Device assembly
  1. Electrode array over a translucent wafer manufacturing (lithography and dicing).
  2. Cover it with an enough thin Teflon layer for EWOD applications (480nm).
  3. Select the suitable gasket for bacteria tests, define UV-curing times and sealing tests.
- Measurements
  1. Numerical simulations, COMSOL complemented to MATLAB calculation for the smeared-out sphere approximation. (DEP behaviour)
  2. Experimental tests, CA measurements and waveform tests in an basic EWOD setup to predict the behaviour in a the chip setup (open wire-free design).
  3. Bacteria tests, in cooperation with KA, microbiology department Salmonella Typhimurium tests were made on PBS and M9 medium with EP and DEP results. Not adhesion was noticed.

## 5.2 Outlook

In this part some future ideas and propositions are exposed; jointly with the conclusion, further studies and projections are being discussed.

The structure of the diced wafer were OK, but during the etching process some electrodes width changed radically. New stable and good structured electrode array can be done with more time in the cleanroom.

Although DEP experiments to avoid biofilms were not taken place, more tests should be made it at different frequencies, as it has been seen in the simulations different forces networks appeared as a result of the electrical field exerted on the medium. This fixed frequencies can be (100Hz, 1kHz, 100kHz) due to their deep changes on EWOD and also on bacteria. It has been modelled, but some tests on resistance of the materials used can give the project more tools for next generations of anti-fouling techniques, mainly a curve of impedance versus voltage and impedance versus frequency to narrow the frequency range simulated on the numerical simulations section.

# Bibliography

- [1] L. Li and D. Uttamchandani, “A concept of moving dielectrophoresis electrodes based on microelectromechanical systems (mems) actuators,” *Progress In Electromagnetics Research Letters*, vol. 2, pp. 89–94, 2008.
- [2] N. Lewpiriyawong, K. Kandaswamy, C. Yang, V. Ivanov, and R. Stocker, “Microfluidic characterization and continuous separation of cells and particles using conducting poly(dimethyl siloxane) electrode induced alternating current-dielectrophoresis,” *Analytical Chemistry*, vol. 83, no. 24, pp. 9579–9585, 2011.
- [3] W. R. on Infectious Diseases, “Factors contributing to resistance,” report, World Health Organization, 2000.
- [4] Department of Communicable Disease, Surveillance and Response, *Prevention of hospital-acquired infections*. World Health Organization, 2nd ed., 2002.
- [5] World Health Organization, *Public Health Importance of Antimicrobial Resistance*, 2014.
- [6] M. Y. Y. Lai, P. K. C. Cheng, and W. W. L. Lim, “Survival of severe acute respiratory syndrome coronavirus,” *Clinical Infectious Diseases*, vol. 41, no. 7, pp. e67–e71, 2005.
- [7] C. for Antimicrobial Resistance in Foodborne Pathogens, *Beyond Antimicrobial Growth Promoters in Food Animal Production*. World Health Organization, who/cds/cpe/zfk/2003.1a ed., November 2002.
- [8] World Health Organization, *Emergence and Spread of Antimicrobial Resistance*, 2014.
- [9] A. C. on Occupational Health Task Force on Infection Control, *Recommendations for Infection Control for the Practice of Anesthesiology*. American Society of Anesthesiologists (ASA), third ed., August 2011.
- [10] ECIS, Electric Cell-substrate Impedance Sensing, *ECIS Cultureware Disposable Electrode Arrays*. Applied BioPhysics, Inc., 2013.
- [11] Teleflex, Arrow, EZ-IO, OnControl and Vidacare registered trademarks, *Arrowgard Clinical Bibliography*. 2014 Teleflex Incorporated, 2011.
- [12] J. B. C. V. L. P. Surman-Lee, ed., *LEGIONELLA and the prevention of legionellosis*, no. ISBN 92 4 156297 8 in WHO Library Cataloguing-in-Publication Data, World Health Organization, WHO Press, 2007.

## BIBLIOGRAPHY

---

- [13] P. C. Hiemenz and R. Rajagopalan, *Principles of Colloid and Surface Chemistry, revised and expanded*, vol. 14. CRC Press, 1997. Page 499.
- [14] N. Jokilaakso, *A Biotechnology Perspective on Silicon Nanowire FETs for Biosensor Applications*. Doctoral thesis, comprehensive summary (other academic), KTH, Protein Technology, November 2013. QC 20131111.
- [15] E. Salonen, “Colloidal interactions and the dlvo theory.” Introduction to Soft Matter Physics (Tfy-3.363) course slides, September 2007.
- [16] W. B. Russel, D. A. Saville, and W. R. Schowalter, *Colloidal dispersions*. Cambridge university press, 1992.
- [17] P. Kaali, E. Strömberg, and S. Karlsson, “Prevention of biofilm associated infections and degradation of polymeric materials used in biomedical applications,” *Biomedical Engineering, Trends in Materials Science, AN Laskovski, Ed., InTech: Rijeka*, pp. 513–540, 2011.
- [18] R. Dickinson, A. Ruta, and S. Treusdal, “Physicochemical basis of bacterial adhesion to biomaterial surfaces,” *Antimicrobial/Anti-Infective Materials*, vol. 1, 2000.
- [19] H. A. Pohl, “The motion and precipitation of suspensoids in divergent electric fields,” *Journal of Applied Physics*, vol. 22, pp. 869–871, July 1951.
- [20] R. Oliveira, J. Azeredo, P. Teixeira, and A. Fonseca, “The role of hydrophobicity in bacterial adhesion,” *University of Minho/Hydrophobicity and adhesion*, 2001.
- [21] K. Khoshmanesh, S. Nahavandi, S. Baratchi, A. Mitchell, and K. Kalantar-zadeh, “Dielectrophoretic platforms for bio-microfluidic systems,” *Biosensors and Bioelectronics*, vol. 26, no. 5, pp. 1800 – 1814, 2011.
- [22] A. G. Banpurkar, K. P. Nichols, and F. Mugele, “Electrowetting-based microdrop tensiometer,” *Langmuir*, vol. 24, no. 19, pp. 10549–10551, 2008. PMID: 18720997.
- [23] C. F. Carlborg, T. Haraldsson, K. Oberg, M. Malkoch, and W. van der Wijngaart, “Beyond pdms: off-stoichiometry thiol-ene (oste) based soft lithography for rapid prototyping of microfluidic devices,” *Lab Chip*, vol. 11, pp. 3136–3147, 2011.
- [24] H. I. C. P. A. C. (HICPAC), *Guideline for infection control in health care personnel*. Centers for Disease Control and Prevention Public Health Service, U.S. Department of Health and Human Services, CDC Personnel Health Guideline, vol 26, num 3 ed., 1998.
- [25] R. E. Perez-Roa, D. T. Tompkins, M. Paulose, C. A. Grimes, M. A. Anderson, and D. R. Noguera, “Effects of localised, low-voltage pulsed electric fields on the development and inhibition of pseudomonas aeruginosa biofilms,” *Biofouling*, vol. 22, no. 6, pp. 383–390, 2006. PMID: 17178571.
- [26] K. R. V. (1942-), *Electric properties of blood and impedance cardiography*. 44.86 hematologie, Rijksuniversiteit Groningen, Proefschrift Groningen Met lit. opg. en samenvattingen in het Nederlands en Duits, 1992. 106 p.

## BIBLIOGRAPHY

---

- [27] S. Mohapatra, K. Costeloe, and D. Hill, "Blood resistivity and its implications for the calculation of cardiac output by the thoracic electrical impedance technique," *Intensive Care Medicine*, vol. 3, no. 2, pp. 63–67, 1977.
- [28] J. H. Long, "The electrical conductivity of urine in relation to its chemical composition," *Journal of the American Chemical Society*, vol. 26, no. 1, pp. 93–105, 1904.
- [29] S. B. Kumar, K. Mathew, U. Raveendranath, and P. Augustine, "Dielectric properties of certain biological materials at microwave frequencies," *The Journal of microwave power and electromagnetic energy: a publication of the International Microwave Power Institute*, vol. 36, no. 2, pp. 67–75, 2001.
- [30] S. Lindsay, *Introduction to Nanoscience*. ISBN:978-019-954420-2, Great Clarendon Street, Oxford OX2 6DP: OUP Oxford, 2009.
- [31] Y.-C. Kim, "Diffusivity of bacteria," *Korean Journal of Chemical Engineering*, vol. 13, no. 3, pp. 282–287, 1996.
- [32] T. Kalwarczyk, M. Tabaka, and R. Holyst, "Biologisticsdiffusion coefficients for complete proteome of escherichia coli," *Bioinformatics*, vol. 28, no. 22, pp. 2971–2978, 2012.
- [33] K. Dill and S. Bromberg, *Molecular Driving Forces: Statistical Thermodynamics in Chemistry and Biology*. ISBN: 0815320515, 9780815320517, Garland Science, 2003.
- [34] R. B. Bird, W. E. Stewart, and E. N. Lightfoot, *Transport phenomena*. John Wiley & Sons, 1976.
- [35] M. Dhindsa, S. Kuiper, and J. Heikenfeld, "Reliable and low-voltage electrowetting on thin parylene films," *Thin Solid Films*, vol. 519, no. 10, pp. 3346 – 3351, 2011.
- [36] N. C. f. E. Division of Healthcare Quality Promotion (DHQP) and Z. I. D. (NCEZID), *Sterilization or Disinfection of Medical Devices*. Centers for Disease Control and Prevention, 1998.
- [37] S. Department of Communicable Disease and Response, "Infection prevention and control of epidemic- and pandemic-prone acute respiratory diseases in healthcare." webpage, May 2007.
- [38] Cathay General Hospital, *Home care for trachea treatment patients*. Cathay Financial Holding Co., Ltd., 2011.
- [39] M. L. Hemani and H. Lepor, "Skin preparation for the prevention of surgical site infection: which agent is best?," *Reviews in Urology*, vol. 11, no. 4, p. 190, 2009.
- [40] D. of Blood Safety and C. Technology, *Surgical care at the district hospital*. World Health Organization 2003, 20 Avenue Appia, 1211 Geneva 27, Switzerland, isbn 92 4 154575 5 ed., September 2003.
- [41] G. H. O. (GHO) and N. diseases (NCD), eds., *The local small-scale preparation of eye drops*, WHO/PBL/01.83, World Health Organization, Vision 2020 actionplan, 2002.

## BIBLIOGRAPHY

---

- [42] S. Z. Yoon, Y.-S. Jeon, Y. C. Kim, Y. J. Lim, J. W. Ha, J. H. Bahk, S. H. Do, K. H. Lee, and C. S. Kim, “The safety of reused endotracheal tubes sterilized according to centers for disease control and prevention guidelines,” *Journal of Clinical Anesthesia*, vol. 19, no. 5, pp. 360 – 364, 2007.
- [43] Tapia-Jurado&Reyes-Arellano&Garca-Garca&Jimnez-Corona&Pea-Jimnez and Len, “Comparison of cost/effectivity of surgical wash with various antiseptics,” *CIRUGA Y CIRUJANOS*, vol. 79, no. 5, pp. 415–420, 2011.
- [44] D. of Diarrhoeal and A. R. D. Control, *Guidelines for the control of epidemics due to Shigella dysenteriae type 1 (Sd1)*. World Health Organization, 1994.
- [45] J. Berthier, P. Clementz, O. Raccurt, D. Jary, P. Claustre, C. Peponnet, and Y. Fouillet, “Computer aided design of an {EWOD} microdevice,” *Sensors and Actuators A: Physical*, vol. 127, no. 2, pp. 283 – 294, 2006. ;ce:title;MEMS 2005 Special Issue;/ce:title; ;ce:subtitle;Special Issue of the Micromechanics Section of Sensors and Actuators (SAMM), based on contributions revised from the technical digest of the {IEEE} 18th International Conference on Micro Electro Mechanical Systems (MEMS-2005).;/ce:subtitle;.
- [46] J. J. Pak, “Simplified ground-type single-plate electrowetting device for droplet transport,” *Journal of Electrical Engineering & Technology*, vol. 6, no. 3, pp. 402–407, 2011. Publisher : The Korean Institute of Electrical Engineers.

## Appendix A

# Biofilm on hospital environments challenges

In order to consider a surface disinfected, a chemical procedure (germicide) must be used to eliminate all pathogenic microorganisms. From the three existing levels, the highest kills all bacteria present by sterilants, the intermediate kills most of viruses, and bacteria by “tuberculocide” (the killing of tuberculosis bacilli); and the lowest level kills only some viruses and bacteria by hospital disinfectants.

One short step before disinfection is always cleaning the surfaces to rise the germicide effect.[36]. This carry on costs on disinfectants (hypochlorite, quaternary ammonium), laundry, technical personal training, waste management as it is described in the infection prevention manual from World Health Organization (WHO)[37]. In addition it must be taking on count different disinfection protocols and disinfectants worldwide (upon the period of time needed to disinfect, known as “contact times”) which also can lead to material degradation problems if is not correctly used (i.e. the rubber cracking caused by several alcohol applications) Annex H in [37].

On top of that high-level disinfection for semi critical items also add costs like sterilization equipment (autoclave, ethylene oxide EO gas sterilizer) which are not compatible with all used medical materials neither, Annex J in [37]. But if home care is required like Trachea tube sterilization, it needs to be sterilized until three times a day if necessary, where also needs to be disassembled, sterilize for a period of time (high temperature) and reassembled again for use it[38]. Preoperative skin preparation is also critical, where common disinfectant agents are less probable effective due to evaporation, neglected hair removal and non-uniform results over the covered area[39]. Wound healing can be impaired by infection if it is not prevented; bacteria cannot be eliminated but is reduced by aseptic measures. Disinfections’ solutions only inactivate infections agents and sterilization kills microbes[40].

Even in very common prosthetics like contact lenses, autoclave, high pressure chambers and steamers are needed by specialists to sterilize them and eye drops; they are also working with antimicrobial agents like gentamicin, neomycin and povidone iodine when autoclaving cannot be done which can lead to skin irritation or a basic knowledge of administration doses[41].

A latent problem in developing countries is the way to reuse daily sterilized endotracheal tubes (ETTs) to reduce the hospital costs. As a consequence, Centers for Disease Control

---

(CDC) guidelines sterilizations methods as ethylene oxide gas (EO) or alkaline glutaraldehyde (GA) solution may affect the mechanical properties of tube's material(mainly the ETT's cuff), specifically the tensile strengths as a result of continue reprocess of them[42].

It can be seen that costs vary from more than 5 Euros up to 20 only in washing hands, Table 5 in [43]. Antimicrobials need to be administrated more than once, and for a period of time to have an effect, and depending on the variation of it can be more sensitive to store and transport to others, Table 1 in [44]. Consequently depending on the used antiseptic some advantages or disadvantages can be pop out: alcohol can have a immediate effect but would produce skin irritation or dryness, on the contrary hexachlorophene can have good effect but it takes more time to act), Table 6 in [43].

Another fact to be taking on consideration is the period of time the material to disinfect are in used, like Legionnaires' disease patients needed more than others. [12]



# Appendix B

## MATLAB Program

In this part all program code is written.

### B.1 Command set

Program code is completely shared.

```
clear all;
j = sqrt(-1);
%E permittivity, cE complex permittivity
%cE = compl_permt(e, s, w)
% e = permittivity (F/m)
% s = conductivity (S/cm)
% w = angular frequency (Hz)
%e0 = 8.8542e-12;%vacuum permittivity (F/m)
% %w=1.3; % Khz Specific frequency
%
f=10*106;
%f = logspace(2,8,1000); % Hz frequency range
w = 2*pi*f; % angular frequency range
%-----
%YEAST - 3 layer
%Radius from inner to outer (1...)
r1 = 2.35*10-6;%particle inner radius (m)
r2 = 2.36*10-6;%particle middle radius (m)
r3 = 2.50*10-6;%particle outer radius (m)

%Conductivity from inner to outer (1...)
sr1 = 2*10-1;%particle inner radius conductivity(S/m)
sr2 = 25*10-8;%particle middle radius conductivity(S/m)
sr3 = 140*10-4;%particle outer radius conductivity(S/m)

%Permittivity from inner to outer (1...)
```

## B.1 Command set

---

```
er1 = 60*e0;%particle inner radius permittivity(F/m)
er2 = 6*e0;%particle middle radius permittivity(F/m)
er3 = 50*e0;%particle outer radius permittivity(F/m)

%Particle Permittivity (bacteria) - calculation
%complex permittivity by layers
ce1 = compl_permt(er1, sr1, w);
ce2 = compl_permt(er2, sr2, w);
ce3 = compl_permt(er3, sr3, w);

%complex permittivity between layers 1&2
CM21 = (ce1-ce2)./(ce1+2*ce2);
r21 = r2/r1;
ce21 = ce2.*(((r21^3)+2*CM21)./((r21^3)-CM21));

%complex permittivity between layers 3&21 (particle)
CM321 = (ce21-ce3)./(ce21+2*ce3);
r32 = r3/r2;

cep = ce3.*(((r32^3)+2*CM321)./((r32^3)-CM321));

%-----
%-----
%MEDIUM (water)
%sm = 2*10^4;%medium conductivity (S/m)% 2(uS/cm) DI water
sm = 38000*10^-6;%medium conductivity (S/m)%from COMSOL, wikipedia
em = 80*e0;%medium permittivity (F/m)
cem = compl_permt(em, sm, w);
% Clausius-Mossotti factor
CM = (cep-cem)./(cep+2*cem);
output = real(CM);
%semilogx(f,output);
%xlabel('frequency (Hz)');
%ylabel('Re[K(w)]');
%grid on;
%////////////////////////////////////
%////////////////////////////////////
%-----
%E. COLI - 3 layer
%Radius from inner to outer (1...)
r1b = 0.975*10^-6;%particle inner radius (m)
r2b = 0.98*10^-6;%particle middle radius (m)
r3b = 1*10^-6;%particle outer radius (m)

%Conductivity from inner to outer (1...)
```



## Appendix C

# COMSOL simulations

In this part extra information from the simulations are shown.

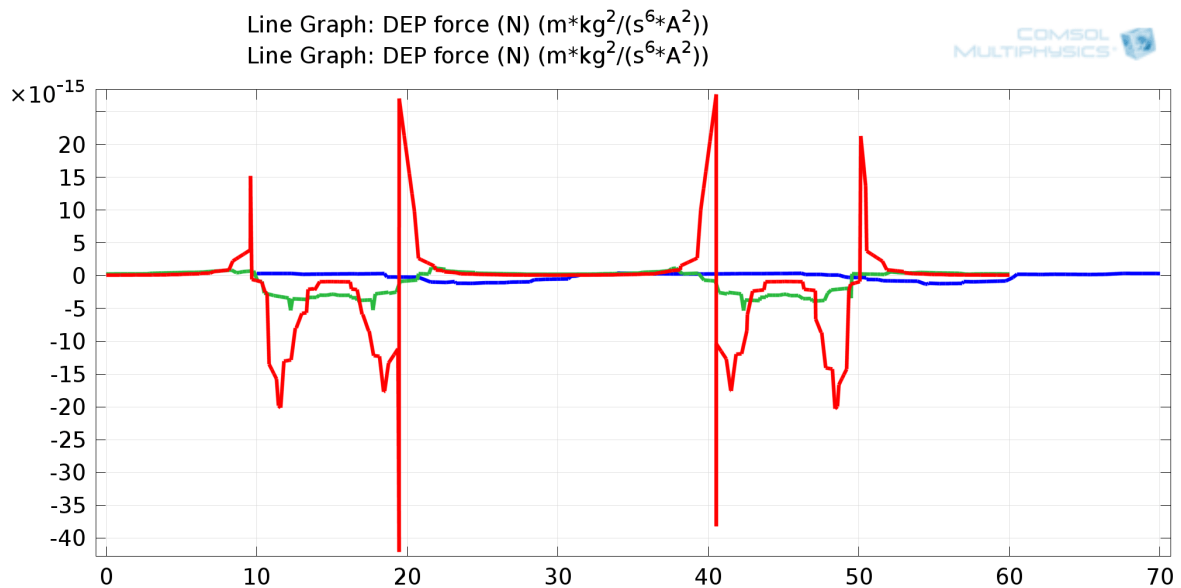


Figure C.1: DEP forces at different heights, 7  $\mu\text{m}$  (blue), 3  $\mu\text{m}$  (green), 1  $\mu\text{m}$  (red) above electrodes (21-29 and 51-59  $\mu\text{m}$  in x-axis)

## Appendix D

# Bacteria formation

In this part further information of the bacteria and results are exposed, which can be divided in the particle and its floating medium.

### D.1 Bacteria

In this part the biological information and results are set out.

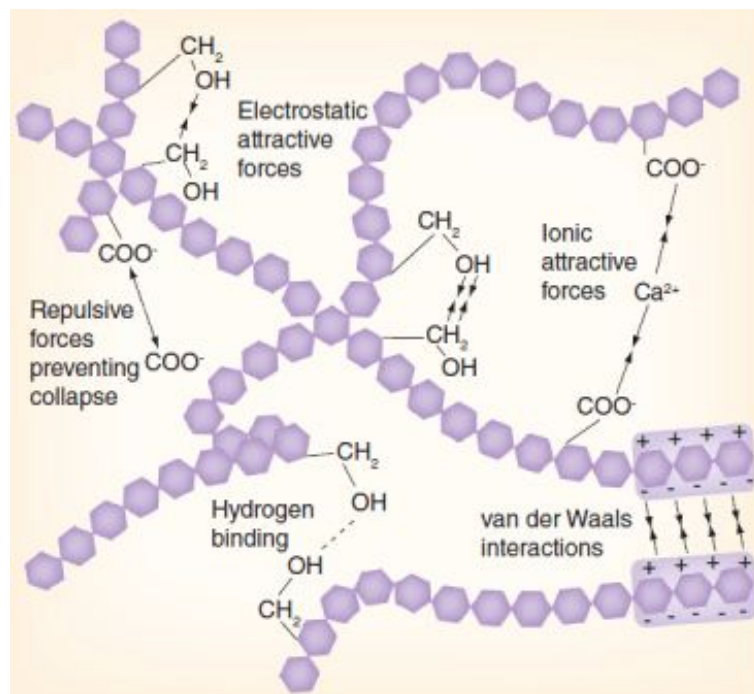


Figure D.1: Bacteria biofilm internal bonding forces

## D.2 Medium

In this part medium characteristics are mentioned.

| (5x)          | M9 medium | 1l                 |
|---------------|-----------|--------------------|
| 168 $\mu$ mol | 37.6g     | $Na_2HPO_4 - H_2O$ |
| 110 $\mu$ mol | 15g       | $KH_2PO_4$         |
| 94 $\mu$ mol  | 5g        | $NHO_4Cl$          |
| 43 $\mu$ mol  | 2.5g      | $NaCl$             |

| (1x)            | M9 medium    | 500ml        |
|-----------------|--------------|--------------|
|                 | 100mL        | 5xM9         |
| 10 $\mu$ mol    | 5mL          | Glucose(1M)  |
| 1 $\mu$ mol     | 500 $\mu$ L  | $MgSO_4$     |
|                 | 25 $\mu$ L   | Thiamin(1%)  |
| 0.027 $\mu$ mol | 13.5 $\mu$ L | $CaCl_2(1M)$ |
|                 | 400mL        | $H_2O$       |

Table D.1: M9 medium parameters and dilution

## Appendix E

# OSTE tests detailed information

In this part OSTE properties and information is delineated.

### E.1 Material specification

In this part all materials used on the OSTE are considered and displayed.

From Sterilin.co.uk is obtained the following information:

| Item Code | Description                | Well Capacity( $\mu$ L) | Material | Sterility |
|-----------|----------------------------|-------------------------|----------|-----------|
| 611F96    | 96 well plate, Flat bottom | 400                     | PS       | NS        |

Table E.1: Culture plate information from catalogue(Microtitre Plates, Clear from Sterilin <http://www.sterilin.co.uk/>)

## Appendix F

# Chip fabrication detailed information

In this part further information about glass wafer electrodes manufacturing is laid out in different scenarios.

### F.1 Design / L-EDIT

In this part, first attempts of designs are described and explained why they could not work.

Even with the choice on hand to use the interdigitated array for the electrodes many topologies came to pop up and the simplest one was chosen. FigF.1

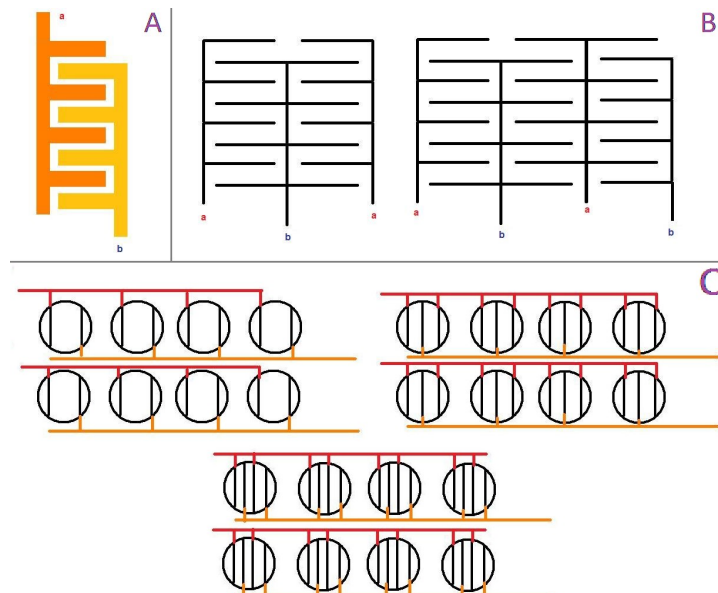


Figure F.1: Different designs for the electrode array topology: (A)basic array, (B) tree array and (C)top-bottom tree array



Since in every test the most important aim to is try to use as much as the it could be the resources that we count on; the first attempt of the design was thought to cover almost all the wafer in order to have more test areas FigF.2; but later on, the cost by each wafer make me to re-design the mask and maximized the area to be used in a (10 mm) diameter wafer, 9 interdigitated electrodes are chose to be fit in a quarter of wafer.Fig3.2b

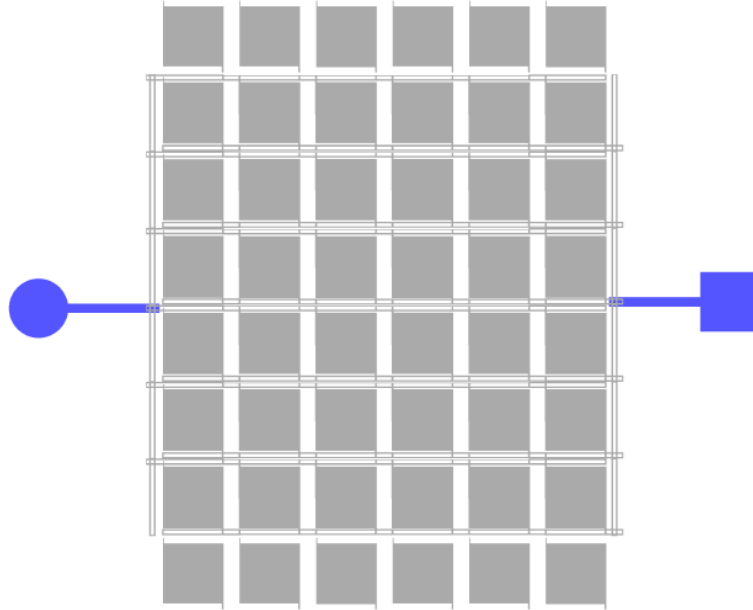


Figure F.2: First attempt to design the wafer mask allowing to have more test spaces.

## F.2 Procedures

In this part, a more detailed information about the procedures used in the lithography process which are too redundant to be in the thesis.

Feedback from the lithography was useful to not “overcured” the lithography by applying too much intensity of light or too much time under the UV exposure.

Such process can be shown in Fig.fig:etchingProb.

Steps:

- nLOF: spin speed 3000 RPM for 30s
- soft bake 110°C for 60s
- exposure for 22s: 440mJ/cm<sup>2</sup>
- Dev: MST AF 4in Dev nLOF 2070 (loaded recipe)

First attempt on lithography:

Coating sample was a proportion of *AZ nLOF 2035:RER600* by (2:1) prepared on the year 2010. This coating was spun at 3000 RPM for 30 s.

### F.3 Parameters

---

It has been made 4 attempts with different UV exposures and development periods as it can be seen on Table F.1 and Table F.2. The type of contact was 'Lo Vac' with a Al.Gap( $\mu\text{m}$ ) of 40.

|             | Times on wafer |             |         |       |
|-------------|----------------|-------------|---------|-------|
|             | 1st            | 2nd         | 3rd     | 4th   |
| UV exposure | 40 s           | 80 s        | 120 s   | 80 s  |
| Development | 3+1+2+3 min    | 3+2+4+5 min | 5+4 min | 5 min |

Table F.1: UV exposure and development times - Second lithography attempt with standard softbake( $110^{\circ}\text{C}$ )

| Second attempt | Times on wafer |  |         |                                 |      |
|----------------|----------------|--|---------|---------------------------------|------|
|                | 1st            | 2nd  | 3rd     | 4th (more intense UV, ch2[20W]) | 5th  |
| UV exposure    | 10 s           | 5 s  | 8 s     | 10 s                            | 10 s |
| Development    | 3+1+2+3 min    | 3+2+4+5 min  | 5+4 min | 5 min                           | -    |
|                | handmade       | Maximus 804 ATM sse (Coating and develop of PR film) |         |                                 |      |

Table F.2: UV exposure and development times - Second lithography attempt with lower softbake( $90^{\circ}\text{C}$ )

| Times of UV exposure by Tab.F.2 |                            |       |   |       |   |       |
|---------------------------------|----------------------------|-------|---|-------|---|-------|
|                                 |                            | 5 s   |   | 8 s   |   | 10 s  |
| # 1 (in $\mu\text{m}$ )         | Whole gap (2 gaps 1 elect) | 10,67 | > | 10,18 | > | 9,69  |
|                                 | Electrode width            | 4     | < | 4,76  | < | 4,98  |
|                                 | Elec-bus gap               | 5,42  | > | 4,76  | > | 4,60  |
|                                 | Elec-elec gap              | 3,40  | > | 2,79  | > | 2,13  |
| # 2 (in $\mu\text{m}$ )         | Whole gap (2 gaps 1 elect) | 20,52 | > | 20,03 | > | 19,37 |
|                                 | Electrode width            | 8,50  | < | 9,03  | < | 10,02 |
|                                 | Elec-bus gap               | 6,57  | > | 5,91  | > | 4,76  |
|                                 | Elec-elec gap              | 6,30  | > | 5,66  | > | 5,01  |
| # 3 (in $\mu\text{m}$ )         | Whole gap (2 gaps 1 elect) | 55,55 | > | 50,73 | > | 49,25 |
|                                 | Electrode width            | 17,90 | < | 19,05 | < | 20,19 |
|                                 | Elec-bus gap               | 6,40  | > | 5,58  | > | 4,43  |
|                                 | Elec-elec gap              | 16,64 | > | 15,76 | > | 14,70 |

Table F.3: Measurements of the electrodes and gaps in the second attempt from Tab.F.2

### F.3 Parameters

In this part some parameters that are worth to be kept but are not fundamental to be shown. Some parameters of the dicing blades are described.

## F Chip fabrication detailed information

---

Some other parameters that are worth to mention, like Dicing blade measurements illustrated in Table.F.4.

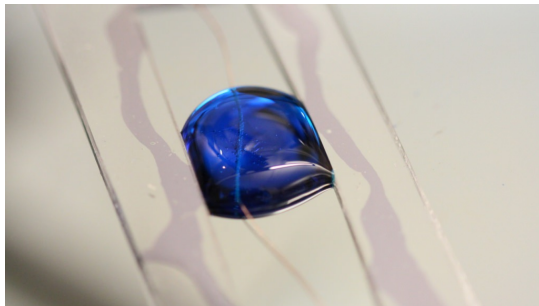
|                     | OD(Out diameter) | Flange diameter (mm) | Blade exposure | Blade thickness (mm) |
|---------------------|------------------|----------------------|----------------|----------------------|
| P1A851 Flange       | 56               | 50,3                 | 2,85           | 0,3                  |
| 27HEEE Hub (Flange) | 56               | 50,3                 | 0,89           | 0,3                  |

Table F.4: Dicing blade parameters about the used Flange

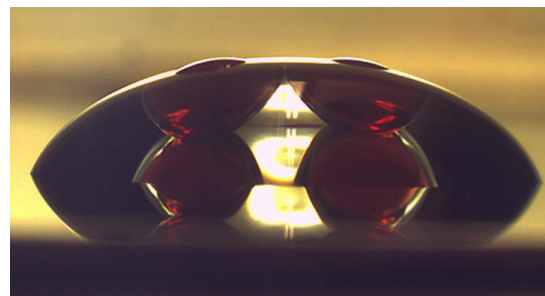
## Appendix G

### EWOD attemps

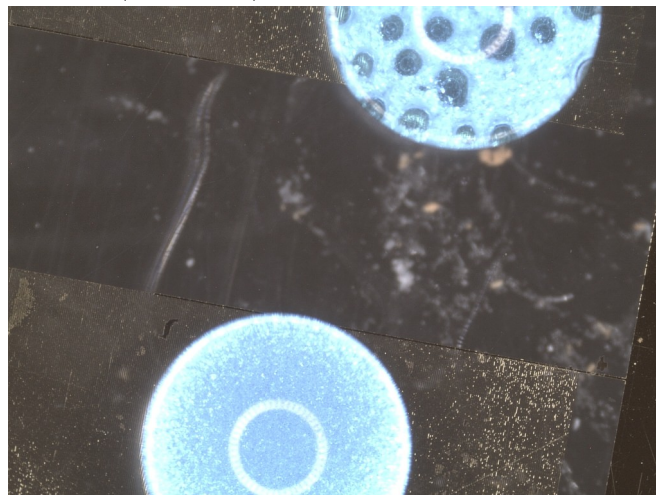
Another test run followed but the idea of DEP on catena[45, 46]. For the powder tests is that used Iridin® 120, Lustre Satin colored (fluid flow flakes) which its particles size is in the range of 5 - 25  $\mu\text{m}$ . It was provided by Mathias Kvik and Fredrik Lundell from the Microluidics laboratory, Wallenberg Wood Science Center, Department of Mechanics, KTH.



(a) Catena test on gasket(copper wire)



(b) Merge of droplets tests



(c) Electrolysis and powder tests

Figure G.1: EWOD variety test